Title

DNA-binding determinants and cellular thresholds for human telomerase repeat addition processivity

Journal

The EMBO Journal, 36(13)

ISSN

0261-4189

Authors

Wu, Robert Alexander
Tam, Jane
Collins, Kathleen

Publication Date

2017-07-03

DOI

10.15252/embj.201796887

Peer reviewed

Article

TRANSPARENT PROCESS

THE EMBO JOURNAL

DNA-binding determinants and cellular thresholds for human telomerase repeat addition processivity

Robert Alexander Wu†, Jane Tam & Kathleen Collins*

Abstract

The reverse transcriptase telomerase adds telomeric repeats to chromosome ends. Purified human telomerase catalyzes processive repeat synthesis, which could restore the full ~100 nucleotides of $(T_2AG_3)_n$ lost from replicated chromosome ends as a single elongation event. Processivity inhibition is proposed to be a basis of human disease, but the impacts of different levels of processivity on telomere maintenance have not been examined. Here, we delineate side chains in the telomerase active-site cavity important for repeat addition processivity, determine how they contribute to duplex and single-stranded DNA handling, and test the cellular consequences of partial or complete loss of repeat addition processivity for telomere maintenance. Biochemical findings oblige a new model for DNA and RNA handling dynamics in processive repeat synthesis. Biological analyses implicate repeat addition processivity as essential for telomerase function. However, telomeres can be maintained by telomerases with lower than wild-type processivity. Furthermore, telomerases with low processivity dramatically elongate telomeres when overexpressed. These studies reveal distinct consequences of changes in telomerase repeat addition processivity and expression level on telomere elongation and length maintenance.

Keywords DNA–RNA duplex; reverse transcriptase; single-stranded DNA; telomerase; telomere maintenance

Subject Categories DNA Replication, Repair & Recombination

DOI 10.15252/embj.201796887 | Received 6 March 2017 | Revised 10 April 2017 | Accepted 11 April 2017 | Published online 11 May 2017

The EMBO Journal (2017) 36: 1908–1927

Introduction

Eukaryotic chromosome ends are capped by tandem simple-sequence repeats, which distinguish stable chromosome termini from inadvertent DNA breaks (Arnoult & Karlseder, 2015). Telomeric repeats provide their end-capping function by recruiting sequence-specific binding proteins that nucleate telomeric chromatin assembly and interactions (Doksani & de Lange, 2014; Martinez & Blasco, 2015; Lloyd *et al*, 2016). In addition, telomeric repeats provide a buffer zone in which a rough balance can occur between sequence loss from incomplete genome replication and sequence gain from *de novo* repeat synthesis (Hockemeyer & Collins, 2015; Greider, 2016). The enzyme capable of *de novo* chromosome end extension is a specialized reverse transcriptase (RT), telomerase (Blackburn *et al*, 2006). Telomerase uses a short region within its integral RNA subunit (TER) as the template for repeat addition to a chromosome 3′ single-stranded overhang primer.

Cellular telomerase holoenzymes are large, multi-subunit assemblies (Wu *et al*, 2017). Some holoenzyme proteins direct TER folding prior to its assembly with the catalytic protein, telomerase reverse transcriptase (TERT). Additional telomerase holoenzyme proteins join the catalytic core RNP to confer and regulate telomerase action at telomeres. The human telomerase holoenzyme contains at least human TER (hTR), two sets of the four-protein H/ACA complex (dyskerin, NHP2, NOP10, GAR1) assembled on the hTR 3′ H/ACA domain, TERT, and the Cajal body localization chaperone TCAB1 (MacNeil *et al*, 2016; Wu *et al*, 2017). Beyond this list of stably associated human telomerase holoenzyme proteins, many more factors contribute to active RNP assembly and trafficking that remain only partially characterized (MacNeil *et al*, 2016; Vasianovich & Wellinger, 2017).

A structurally minimized human telomerase complex can be assembled in extracts such as rabbit reticulocyte lysate (RRL) by expression of TERT and hTR alone. To generate these minimal RNPs, TERT can be combined with full-length hTR (Weinrich *et al*, 1997), two TERT-interacting, activity-essential domains of hTR as separate RNAs (Mitchell & Collins, 2000), or both TERT-interacting domains linked together as streamlined hTRmin (Wu & Collins, 2014). An RRL-reconstituted human telomerase catalytic core has properties of DNA interaction and repeat synthesis that parallel those of the cellular holoenzyme (Zaug *et al*, 2013; Wu & Collins, 2014). Like characterized telomerase enzymes from most organisms, human telomerase copies its internal template with nucleotide addition processivity (NAP) to a specific template 5′ boundary (Podlevsky & Chen, 2016). The 5′ boundary position in telomerase enzymes from single-celled organisms is determined by spacing from a template-flanking RNA–protein or RNA–RNA interaction, but vertebrate telomerases additionally use sequence-specific recognition of the product–template duplex itself to halt template copying after synthesis of a GGTTAG-3′ permutation of the telomeric repeat (Podlevsky & Chen, 2016).

Department of Molecular and Cell Biology, University of California, Berkeley, Berkeley, CA, USA
*Corresponding author. Tel: +1 510 643 1598; E-mail: kcollins@berkeley.edu
†Present address: Department of Biological Chemistry and Molecular Pharmacology, Harvard Medical School, Boston, MA, USA

Purified telomerase holoenzymes or minimal RNPs typically extend a bound primer by multiple repeat additions prior to product dissociation. This repeat addition processivity (RAP) requires nucleic acid dynamics that are unique to telomerase among all reverse transcriptases (Fig 1A): dissociation of the product–template duplex, template repositioning to initiate synthesis from its 3′ end, single-stranded (ss) DNA retention, and active-site stabilization of the short duplex formed at the template 3′ end (Wu *et al*, 2017). It remains an open question how RAP assayed *in vitro* relates to telomere maintenance in cells. *Saccharomyces cerevisiae* telomerase has little if any RAP under diverse assay conditions *in vitro*, but in cells, RAP varies from none to many repeats depending on telomere length (Chang *et al*, 2007). On the other hand, the *Tetrahymena thermophila* telomerase holoenzyme has extremely high RAP *in vitro*, but sequencing of rapidly elongating telomeres in cells co-expressing wild-type and mutant-template TERs suggested limited if any telomerase RAP *in vivo* (Greider, 1991; Yu & Blackburn, 1991). Based on labeled nucleotide incorporation and density gradient centrifugation experiments, human telomerase is proposed to add a uniform ~10 repeats per bound telomere (Zhao *et al*, 2011), which is within the range of human telomerase RAP assayed *in vitro* but much more precise than a typical product length distribution. A chemical inhibitor that reduces human telomerase RAP *in vitro* induces telomere shortening in cells (Damm *et al*, 2001; Pascolo *et al*, 2002), and two disease-causing TERT mutations that compromise RAP suggest decreased RAP as a cause of premature telomere shortening within a human lifespan (Robart & Collins, 2010; Zaug *et al*, 2013). These findings are provocative but do not reveal how much human telomerase RAP is required for telomere elongation or stable length maintenance in cells.

Understanding of the mechanism and structural determinants of telomerase RAP has been elusive. Most studies to date have focused on the TERT N-terminal (TEN) domain. In human TERT (Fig 1B), a proline/arginine-rich linker (PAL) separates the TEN domain from the TERT ring, which contains the high-affinity telomerase RNA binding domain (TRBD), the RT domain, and the C-terminal extension (CTE) analogous to a polymerase thumb domain (Gillis *et al*, 2008; Podlevsky *et al*, 2008; Wu *et al*, 2015). TERT ring RNP without the TEN domain is capable of only single-repeat synthesis, which can be restored to full RAP by addition of a physically separate TEN domain (Robart & Collins, 2011; Wu & Collins, 2014). Recent studies suggest that the TEN domain confers RAP by promoting active-site engagement of the realigned, short template 3′ end duplex (Jurczyluk *et al*, 2011; Wu & Collins, 2014; Akiyama *et al*, 2015). It remains to be understood how telomerase retains single-stranded product DNA without template base-pairing. Much of this interaction could occur within the central cavity of the TERT ring that contains the active site, because RAP of a minimal telomerase RNP does not require ssDNA beyond the length of the initial primer-template duplex (Hardy *et al*, 2001; Baran *et al*, 2002).

Here, we investigate the determinants of product–template duplex handling and ssDNA retention required for RAP within the active-site cavity of the human TERT ring. Using functional and physical assays, we define protein side chains that contribute to distinct, specific steps of the RAP mechanism. We then determine the biological consequences of reduced or eliminated RAP for human cell telomere length maintenance. Our findings suggest a new biochemical model for DNA handling during RAP and establish its physiological importance for telomere maintenance and telomere length set point.

Results

TERT motifs near the active site contribute to repeat synthesis processivity

We sought to understand the structural underpinnings of RAP contributed by the TERT ring. In particular, we considered side chains in TERT-specific motifs (Fig 1B) with potential to contact either the primer or template strand (Fig 1C) based on the high-resolution structure of *Tribolium castaneum* TERT bound to a model DNA–RNA duplex (Mitchell *et al*, 2010). TERT regions studied here include the loop of the conserved T-motif within the TRBD (hTERT residues 566–572), the thumb loop linking the RT and CTE domains (residues 945–969), and the thumb 3_{10} helix region (α18–α20; residues 970–988) in the CTE (Fig EV1). We also investigated RT-domain motif 3 (residues 658–697) because motif 3 sequence substitutions alter primer use, synthesis rate, and RAP (Xie *et al*, 2010).

We extensively substituted the side chains of these TERT regions and screened for impact on telomerase activity using RRL to express human TERT in the presence of hTRmin (data not shown). Side chains were individually substituted to alanine, except in the

Figure 1. Side chains in the TERT active-site cavity contribute to RAP.

A Schematic of the realignment of RNA template (green) and DNA product (blue) for repeat addition processivity. Duplex base-pairs dissociate (step 1), with ssDNA retention, while the template translocates relative to the active site and product strand. Base-pairing between the product strand and the template alignment region (step 2) forms a new short duplex to be engaged by the active site for next-repeat synthesis.

B Schematic of TERT domain and motif architecture. TERT amino acid substitutions characterized extensively in this work are listed below their encompassing motif.

C TERT active-site motifs of interest in this work are colored within the overall ribbon diagram of *Tribolium* TERT crystallized in complex with a model DNA–RNA duplex (PBD accession code 3KYL; Mitchell *et al*, 2010). Product DNA strand is in blue, and RNA template strand is in green.

D Northern blot detection of hTR copurified with FLAG-tagged wild-type (WT) or mutant TERT after co-overexpression in 293T cells. Note that full-length hTR often migrates as a doublet due to partial folding during denaturing acrylamide PAGE.

E Schematic of the multiple-turnover primer extension assay for telomerase activity. Products were labeled by incorporation of radiolabeled dGTP and resolved by denaturing PAGE.

F Activity of telomerase assembled in 293T cells by co-expression of the indicated FLAG-tagged TERT and hTR, assayed after enzyme enrichment by binding to FLAG-antibody resin. In this and subsequent activity assay panels, the recovery control (RC) is a 5′ end-labeled DNA oligonucleotide added prior to product precipitation and 5′ end-labeled unextended primer was run as a size marker (▸).

Data information: Similar results were obtained in independent experimental replicates.

instances of wild-type alanines, which were substituted with valines, and charged residues, which were tested as side-chain substitutions to the opposite charge (acidic side chains were replaced with lysine and basic side chains with glutamic acid). The initial assay used conventional telomeric-repeat extension of the primer $(T_2AG_3)_3$ with dTTP, dATP, and radiolabeled dGTP. While many

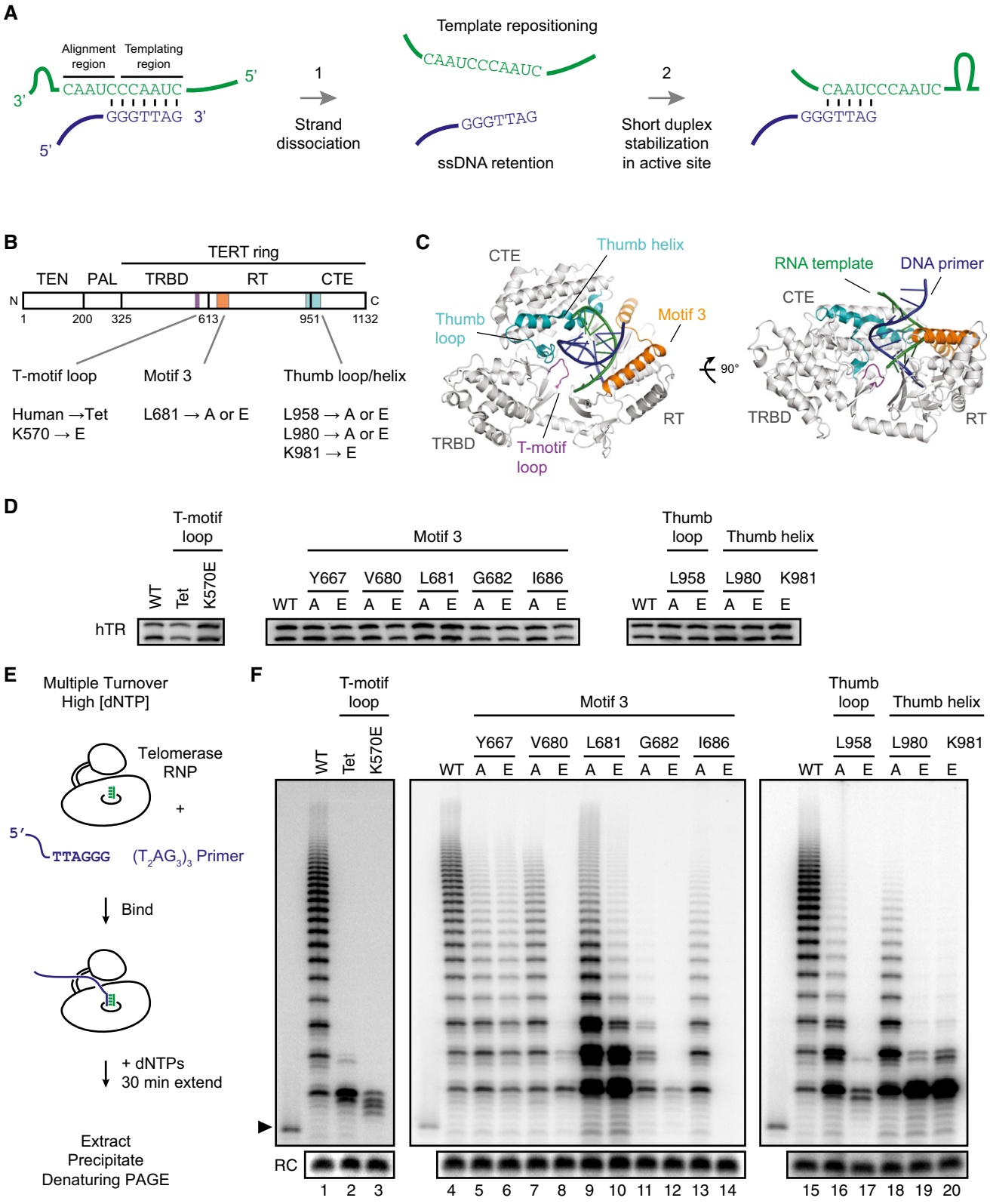

Figure 1.

side-chain substitutions decreased activity in general, we identified nine side chains whose substitution led to relatively selective decrease in RAP: K570 in the T-motif loop; Y667, V680, L681, G682, and I686 in motif 3; and L958, L980, and K981 in the thumb loop or thumb helix.

To further investigate the side chains identified in the initial screen, we assembled telomerase holoenzyme with N-terminally FLAG-tagged wild-type or mutant TERT by transient transfection of human 293T cells. Side chains changed to alanine in the initial screen were also replaced with glutamic acid to exacerbate potential impact on interaction with a nucleic acid backbone. We also replaced the entire seven-residue T-motif loop with the positionally equivalent *Tetrahymena* sequence, because *Tetrahymena* telomerase has substantial RAP but an entirely different T-motif loop sequence (Fig EV1). Thus, swapping the intact loop between the TERTs could preserve RAP. For each of the TERTs reconstituted into telomerase holoenzyme in 293T cells, FLAG-antibody purification of TERT recovered similar amounts of co-expressed hTR (Fig 1D). We conclude that none of the TERT amino acid substitutions substantially compromised RNP assembly.

We first assayed the purified holoenzymes for activity using conventional primer extension with radiolabeled dNTP incorporation (Fig 1E). T-motif loop substitution with the *Tetrahymena* sequence or the single side-chain substitution K570E decreased NAP, evidenced by some products terminated prior to completion of the first repeat, and decreased RAP (Fig 1F, lanes 1–3). RAP was decreased by motif 3 substitutions of Y667, V680, L681, G682, and I686 (Fig 1F, lanes 4–14), largely consistent with conclusions from a previous study of telomerases reconstituted in RRL with TERT Y667A (~75% of wild-type RAP), V680A (~90% of wild-type RAP), L681A (~25% of wild-type RAP), G682A (18% of wild-type RAP), or I686A (35% of wild-type RAP) and holoenzyme reconstituted with TERT G682A (23–25% of wild-type RAP) or I686A (37% of wild-type RAP) (Xie *et al*, 2010). These defects were more severe with the side-chain substitution to glutamic acid than the substitution to alanine (Fig 1F). Mutating thumb-loop/thumb-helix L958 or L980 to alanine decreased RAP, and this decrease was more severe for L958, L980, or K981 substitutions to glutamic acid (Fig 1F, lanes 15–20). Decreased RAP was not correlated with a reduction in product synthesis: motif 3 L681 substitution to alanine or glutamic acid decreased RAP but greatly increased short-product synthesis. Likewise, most of the thumb-loop/thumb-helix substitutions decreased RAP but increased short-product accumulation.

RAP defects in TERT-mutant enzymes are not explained by slow-product release from the template

The initial catalytic-cycle step required for telomerase RAP is dissociation of the product–template duplex (Fig 1A, step 1). Failure of strand separation can be distinguished from a ssDNA retention defect by measuring enzyme turnover (enzyme ability to elongate a different substrate molecule). If the product 3′ end is not readily unpaired from the template, enzyme turnover would decrease. To compare turnover of the TERT-mutant enzymes, we performed a pulse–chase primer extension assay (Fig 2A). Telomerase was first bound to a 27-nucleotide primer provided at 50 nM. This initial primer was extended by telomerase in reactions including radiolabeled dGTP for 5 min. Next, 200-fold molar excess of an 18-nucleotide chase primer was added and DNA synthesis was allowed to continue. Only after telomerase released the initially elongated primer could the chase primer be elongated. The difference in initial and chase primer length ensured that products from their extension were offset. We quantified the accumulation of the single-repeat product of the chase primer over time. To compare across enzymes, we normalized the chase primer product intensity to the initial primer product intensity when the chase was initiated (t = 5 min).

Telomerases with severely reduced RAP due to side-chain substitutions in the T-motif loop (*Tetrahymena* sequence and K570E) or thumb helix (L980E and K981E) had higher turnover than wild-type telomerase, evident in the enhanced accumulation of product from the 18-nucleotide chase primer over the assay time course (Fig 2B and C). The motif 3 L681A and L681E TERT-mutant telomerases also had increased turnover with some processive repeat synthesis (Fig 2B and C). In contrast, the thumb-loop L958E TERT-mutant telomerase with severely reduced RAP did not show increased turnover relative to wild-type TERT telomerase (Fig 2B and C). The relatively normal turnover of severely RAP-compromised L958E TERT telomerase suggests that this enzyme differs from the other RAP-deficient TERT-mutant enzymes in retaining a normal or higher stability of binding to the pre-translocation product–template duplex (see Discussion). In general, the observation that the chase primer was elongated to some extent by all TERT-mutant telomerases suggests that none of them entirely fail to dissociate product–template duplex.

TERT-mutant enzymes retain stimulation by elevated dGTP concentration

Long-product synthesis by human telomerase increases when dGTP concentration is raised well above the physiological dNTP concentration (Maine *et al*, 1999; Sun *et al*, 1999). To investigate whether any of the TERT mutations affected telomerase stimulation by dGTP, we performed activity assays with 5′-radiolabeled primer and unlabeled dNTPs. Radiolabeled $(T_2AG_3)_3$ was bound to telomerase immobilized on antibody resin, unbound primer was removed by washing, and primer extension was initiated by addition of unlabeled dNTPs (Fig 3A). This assay format gave each product an equal radiolabeling intensity and also restricted detectable product synthesis to a single-turnover reaction.

In activity assays with approximately physiological concentrations of dNTPs (10 μM, Fig 3B), wild-type and mutant-TERT enzymes generated profiles of product synthesis similar to those observed with the radiolabeled nucleotide primer extension assay (Fig 1F). The mixture of low-RAP and high-RAP products synthesized by telomerase with L681A TERT was more obvious in the single-turnover assay conditions (Fig 3B, lane 9). Reduced NAP was also sensitized for detection, evident for telomerase enzymes with TERT K570E, V680E, G682E, L958E, or K981E (Fig 3B, lanes 3, 8, 12, 17, and 20).

When the TERT-mutant telomerases were assayed for repeat synthesis in reactions with high dNTP concentration (250 μM, Fig 3C), all of the enzymes had longer products excluding the completely inactive I686E TERT enzyme (Fig 3D). Even TERT

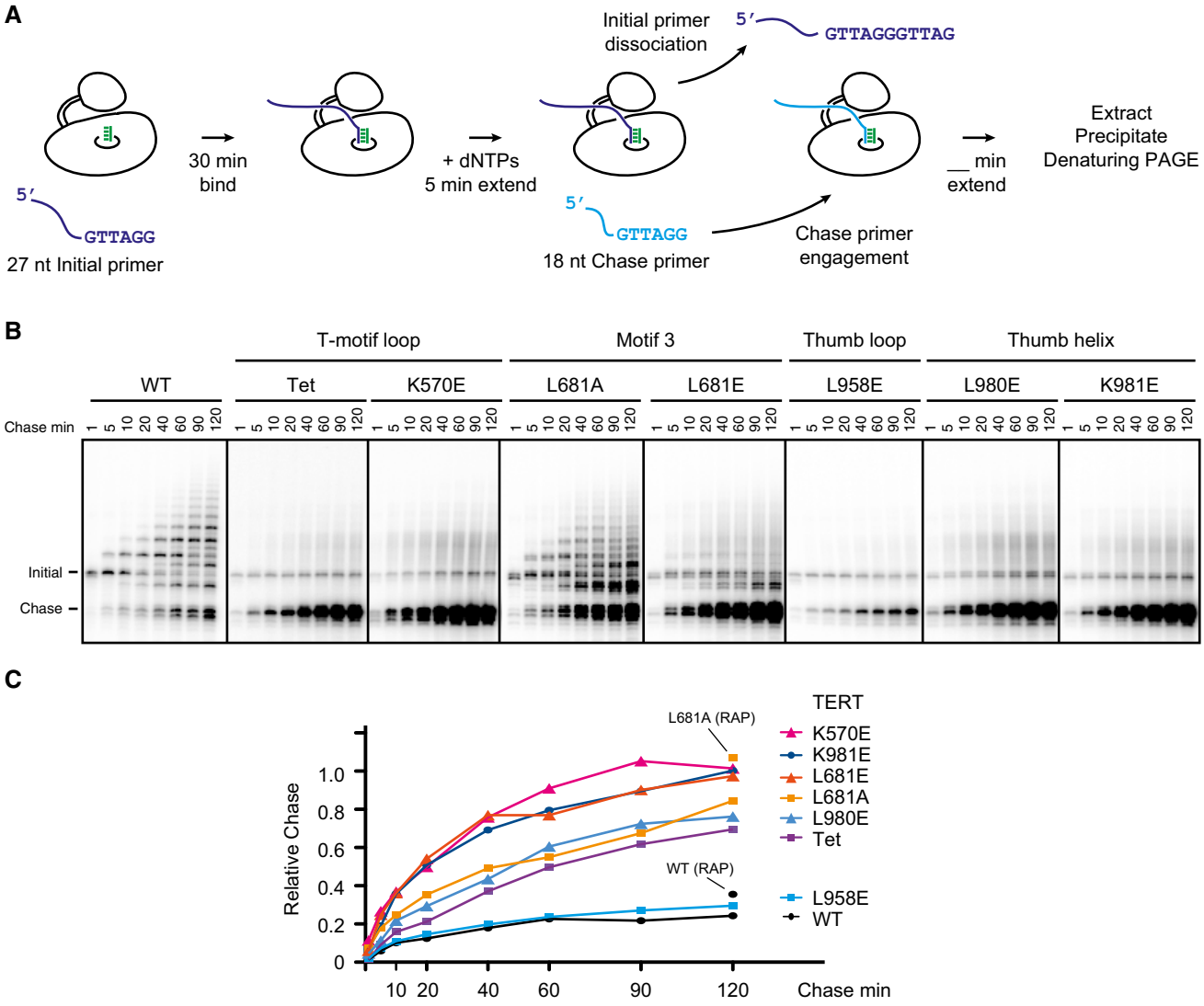

Figure 2. RAP-defective TERT-mutant enzymes retain a wild-type or faster rate of product release.

A Schematic of the pulse–chase primer extension assay. Telomerase immobilized on FLAG-antibody resin was pre-bound with 50 nM of a 27-nucleotide initial primer and labeled during a 5-min incubation with dTTP, dATP, and radiolabeled dGTP. After the pulse labeling, 10 μM of an 18-nucleotide chase primer was added and, upon enzyme dissociation from the elongated initial primer, extended by telomerase.

B Activity of WT and TERT-mutant telomerases at different time points of primer pulse–chase. WT and L681A TERT telomerases retained sufficient RAP to support multiple-repeat extension of the initial and chase primers.

C Quantification of chase primer elongation for the assays shown in (B). The first-repeat addition product was the most abundant of the chase-primer products even for the wild-type enzyme, despite continued elongation of the initial primer over the time course. This difference may be related to the 200-fold higher concentration of chase primer than initial primer present at the time of telomerase engagement. To compare across enzymes, we normalized the chase primer product intensity to the products of the initial primer after the initial pulse labeling. We quantified the predominant first-repeat addition product over time for each enzyme. Values of chase product quantification summing all WT and L681A TERT enzyme products are indicated as isolated symbols at 120-min time point of the assay.

K570E and G682E enzymes with low NAP supported some processive repeat synthesis (Fig 3D, lanes 3 and 12). Of note, relative RAP across the TERT-mutant enzymes remained consistent comparing low-dNTP to high-dNTP reactions. These results indicate that none of the TERT mutations abrogated the increase in processive repeat synthesis with elevated dGTP concentration. Because the stimulatory dGTP is thought to bind in the active site, the lack of change in RAP stimulation supports a "normal" dNTP binding site in the TERT-mutant telomerases.

Nuclease protection of product DNA informs telomerase handing of DNA across the catalytic cycle

We recently developed an assay to monitor physical association of DNA with active telomerase (Wu & Collins, 2014). In this assay (Fig 4A), telomerase elongates a primer with the GTTAGG-3′ end by incorporation of radiolabeled dGTP. After product synthesis, limited digestion with exonuclease VII (ExoVII) trims off the exposed portion of telomerase-bound products and entirely degrades any

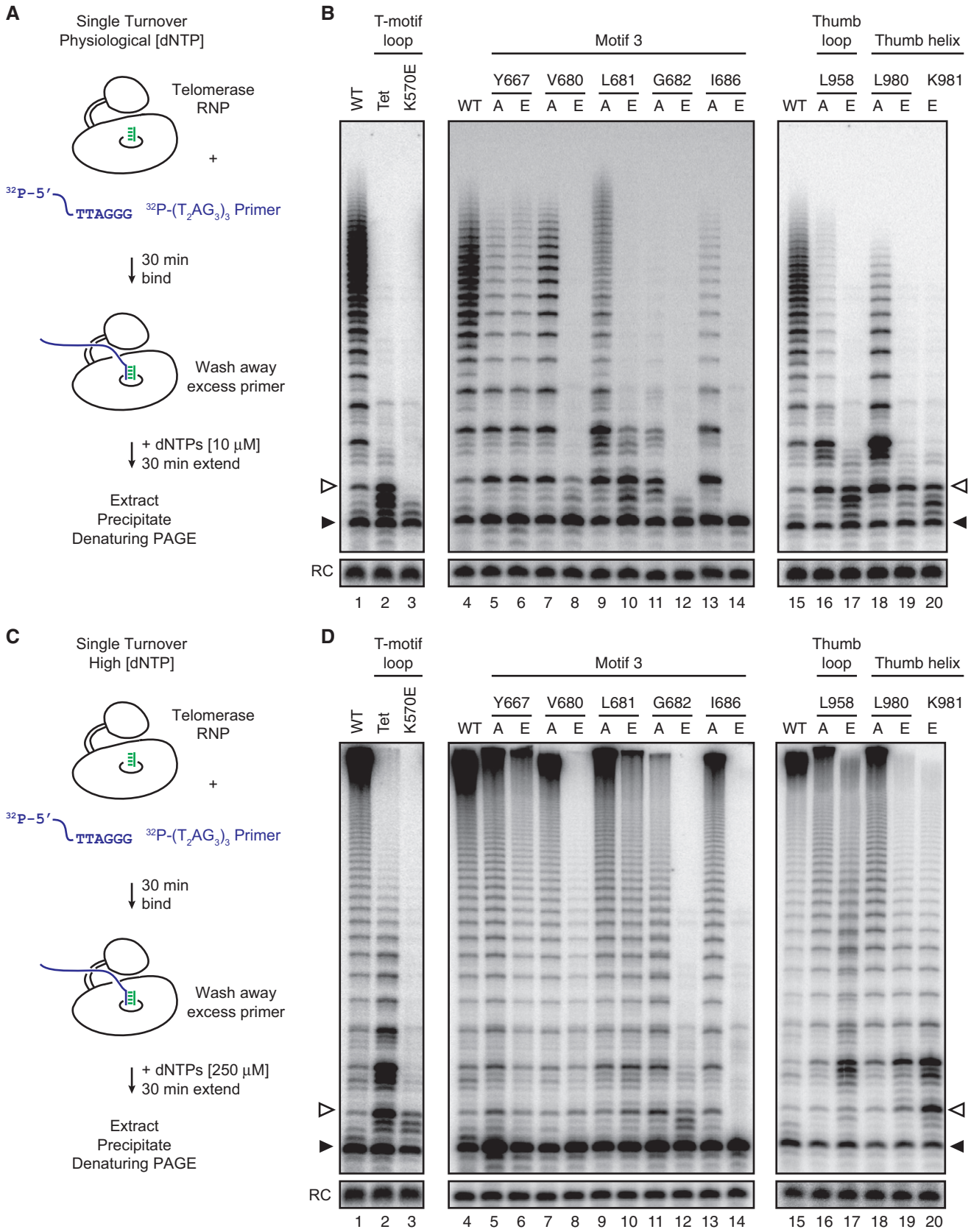

Figure 3.

Figure 3. TERT-mutant telomerases retain the dNTP concentration dependence of RAP.

A Schematic of a single-turnover activity assay of telomerase extending a 5′ end-labeled primer in reactions with approximately physiological levels of dNTPs. The end-labeled primer was pre-bound to telomerase immobilized on FLAG-resin and extended upon addition of 10 μM each dNTP.

B Activity of WT and TERT-mutant telomerases assayed at approximately physiological dNTP concentration. In this and subsequent single-turnover activity assay panels, the completed first repeat is indicated (▸). The product profile in part reflects the limiting amount of dTTP relative to the K_m for dTTP incorporation.

C Schematic of a single-turnover activity assay parallel to (A) but with 250 μM each dNTP.

D Activity of WT and TERT-mutant telomerases assayed at a high-dNTP concentration.

Data information: Similar results were obtained in independent experimental replicates.

released product. Trimmed products are then resolved by denaturing PAGE. Here, as previously, we used the primer T_{21}GTTAGG to avoid sequence-biased exonuclease pausing. Importantly, primers with different 5′ ssDNA sequences have comparable binding to and elongation by human telomerase (Morin, 1991; Wallweber *et al*, 2003; Wu & Collins, 2014). Synthesis can be advanced to specific template positions prior to nuclease addition by varying the combination of dNTPs and ddNTP added to the primer extension reaction (Fig 4B). Previously, we proposed that the length of DNA protected from nuclease digestion reflects a relatively constant length of ssDNA and a varying length of duplex (Wu & Collins, 2014). This hypothesis was based in part on the stepwise increase in protected product length with repeat synthesis by TERT ring RNP. Here, we extended this analysis to monitor the protected products of full-length TERT RNP paused in synthesis at each template position (Fig 4B).

Exonuclease digestion of telomerase holoenzyme products yielded protected lengths of 17–22 nucleotides (Fig 4C; note that the longest radiolabeled DNA corresponds to the full-length, undigested primer extension product). Protected product length profiles suggested that ExoVII digestion often yields a triplet of bands, with a major peak and weaker −1 and +1 nucleotide peaks (Wu & Collins, 2014). We identified the peak in protected product intensity (Fig 4D) using semi-automated footprinting analysis software (SAFA), which deconvolves and quantifies the profile of product intensities using Lorentzian curve fitting (Das *et al*, 2005). Protected product lengths generally increased with synthesis to the template 5′ end (Fig 4D and E). The 18-nucleotide protected product ending in AGGG-3′ increased to 20 nucleotides in length when synthesis extended to GGTT-3′ (Fig 4C and D; note that some of the GGTT-3′ product may be extended by an additional dGTP misincorporation at template U47, which did not mimic matched dNTP addition described below). The gradual increase in protected product lengths is consistent with a monotonic gain in duplex length for every dNTP added (Fig 4E; see below).

In contrast to the monotonic increase in protected product lengths during synthesis across mid-template positions, protected product lengths decreased when synthesis extended to GTTA-3′ (Fig 4C and D). Subsequent addition of the final nucleotide to generate TTAG-3′ gave the typical one-nucleotide increase in protected product length, with peak intensity of protected product at 20 nucleotides, similar to the profile for GGTT-3′ (Fig 4C and D). The departure from a monotonic increase in protected product length was specific for product synthesis to GTTA-3′ across numerous replicates. We suggest that when synthesis reaches GTTA-3′, up to two base-pairs of duplex are favored to dissociate, resulting in a duplex at the template 3′ end that extends only to template C52 (Fig 4E, see below).

The actual extent of human telomerase product–template base-pairing is not directly determined, despite many chemical mapping efforts (data not shown). We therefore investigated the base-pairing status of the alignment region at the template 3′ end indirectly, by nuclease protection profiling after extension of a primer ending in CCCAGG-3′ (Fig 4F). This primer was extended with wild-type RAP (Fig EV2). No dip in protected product length was observed when synthesis stepped to GTTA-3′ (Fig 4F, compare lanes 3–4 to 8–9). Instead, protected product length remained largely the same. These results are consistent with the CCCAGG-3′ primer forming one less initial base-pair with the template prior to extension, and subsequently dissociating only one base-pair with extension from GGTT-3′ to GTTA-3′ instead of the two base-pairs dissociated with a GTTAGG-3′ primer (Fig 4G).

Combined results above lead us to suggest that the product–template duplex increases gradually in length to a maximum of about seven base-pairs (Fig 4E). The gradual increase in duplex length during mid-template synthesis agrees with predictions based on primer base-pairing requirements (Wang & Blackburn, 1997), and the maximum of seven base-pairs matches the duplex length determined by chemical modification of *S. cerevisiae* telomerase paused at two template positions (Förstemann & Lingner, 2005) and predictions from the structure of TERT ring bound to a model DNA–RNA duplex (Mitchell *et al*, 2010). When synthesis reaches GTTA-3′, up to two base-pairs of duplex may preferentially dissociate (Fig 4E). We disfavor the alternative of an ever-increasing duplex length with shortened ssDNA path, because human telomerase product off-rate increases with synthesis from mid-template to the template 5′ end (Wallweber *et al*, 2003).

Some RAP-compromised enzymes have altered DNA–RNA duplex length and/or stability

Next we compared wild-type TERT RNP to TERT-mutant RNPs for differences in nuclease-protected product lengths across repeat synthesis. Enzymes with the motif 3 L681A and L681E substitutions had profiles of nuclease-protected product lengths very similar to the wild-type enzyme (Figs 5A and B, and EV3). In comparison, enzyme with the thumb-loop L958E substitution had a wild-type pattern of nuclease-protected product lengths for synthesis through GGTT-3′ but no decrease in protected product length at GTTA-3′ (Fig 5A and B). Like the L958E TERT enzyme, enzymes with the thumb-helix substitutions L980E and K981E or the T-motif loop substitution to *Tetrahymena* sequence had profiles of product protection with no decrease in protected product length at GTTA-3′, but they also had increased product dissociation with synthesis toward the template 5′ end evident in a loss of intensity of protected products (Figs 5A and B, and EV3). Enzyme with the T-motif loop

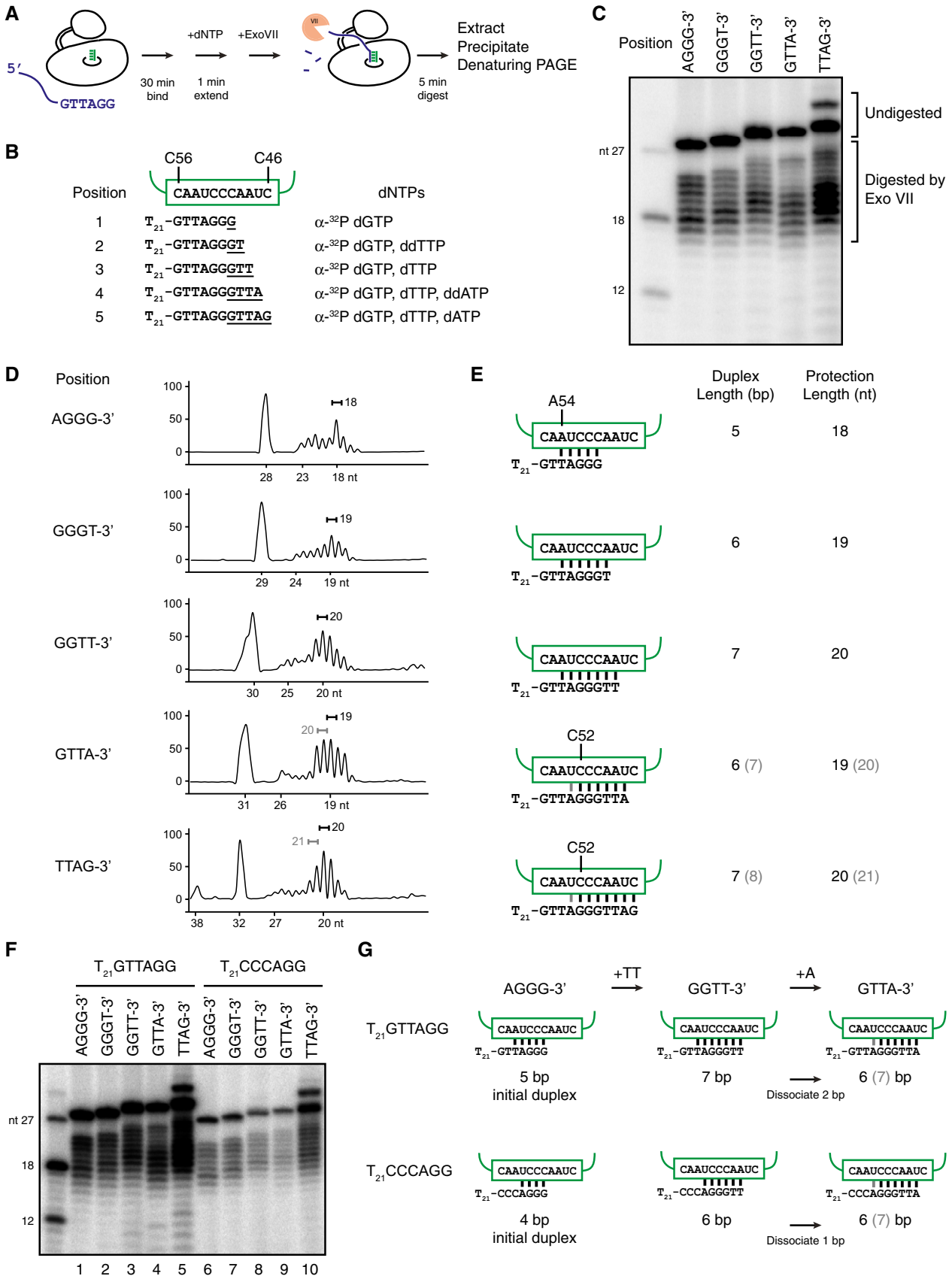

Figure 4.

Figure 4. Nuclease protection detects changing states of enzyme–product interaction.

A Schematic of the nuclease protection assay. The 27-nucleotide DNA primer T_{21}GTTAGG was pre-bound to immobilized telomerase for 30 min and then labeled by telomerase activity for 1 min. The telomerase–DNA complex was then treated with ExoVII for 5 min. The protected, labeled product was extracted, precipitated, and resolved by denaturing PAGE.

B Schematic of repeat synthesis advanced to each template position by addition of specific combinations of dNTPs and ddNTPs. Product synthesis was halted at each position prior to addition of ExoVII.

C ExoVII protection assayed at each step of repeat synthesis for WT telomerase. In this and subsequent nuclease protection assay panels, both undigested and ExoVII-digested telomerase products are observed. Size markers are 5′ end-labeled 27-, 18-, and 12- nucleotide DNA oligonucleotides. Similar results were obtained in independent experimental replicates.

D Protected product profiles from (C) quantified by SAFA. Major and minor product peaks and lengths are indicated in black and gray, respectively.

E Schematic of proposed duplex base-pairing dynamics during repeat synthesis. The extent of nuclease protection (protection length) is modeled as a varying duplex length and a relatively fixed length of ssDNA.

F ExoVII protection assayed at each step of repeat synthesis for WT telomerase elongation of T_{21}GTTAGG or T_{21}CCCAGG primer. Similar results were obtained in independent experimental replicates.

G Model of the changing state of duplex base-pairing as extension proceeds from AGGG-3′ to GGTT-3′ to GTTA-3′ for primers T_{21}GTTAGG and T_{21}CCCAGG.

substitution K570E failed to protect a substantial amount of product DNA at any template position (Figs 5A and EV3), suggesting that its low NAP (Figs 1F and 3B and D) derives from premature product dissociation during repeat synthesis. Loss of product DNA protection correlated with an increase in the amount of radiolabeled DNA fragment running at the leading edge of the gel (Fig 5A).

Overall, these results classify the NAP-proficient, RAP-deficient enzymes into two categories: those with wild-type duplex recognition (the motif 3 TERT-mutant enzymes) and those that fail to transition to duplex unpairing after synthesis of GTTA-3′. This assigns product–template duplex handling function to both the thumb loop and thumb helix (see Discussion). However, the thumb-loop TERT-mutant enzyme had no apparent loss of duplex binding stability, whereas the thumb-helix and T-motif loop TERT-mutant enzymes had increased product release with synthesis toward the template 5′ end. This finding distinguishes the catalytic-cycle functions of the TERT thumb loop versus thumb helix (see Discussion). Because none of the thumb-loop, thumb-helix, or T-motif loop TERT-mutant enzymes had a wild-type enzyme step-back in duplex length upon synthesis to GTTA-3′, we suggest that these motifs have a role in binding template-dissociated ssDNA (see Discussion).

Telomere length maintenance depends on RAP but not wild-type RAP

We exploited TERT mutations that imposed graded extents of RAP deficiency to test the biological significance of human telomerase RAP. For comparison, we selected motif 3 L681E TERT with intermediate RAP and thumb-helix L980A with low RAP assayed in reactions with near-physiological dNTP concentration (Fig 3B, lanes 10 and 18). We also selected TERTs with T-motif loop *Tetrahymena* sequence or thumb-helix K981E substitution that have no RAP at physiological dNTP concentration but modest RAP at elevated dNTP concentration (Fig 3D, lanes 2 and 20).

Homozygous disruption of the endogenous TERT locus ($TERT^{-/-}$) in the pseudo-diploid human HCT116 colon cancer cell line leads to progressive telomere shortening and ultimately cell death induced by critically short telomeres (Vogan *et al*, 2016). Telomerase activity, telomere length, and cell viability can be restored by integration of a TERT expression transgene at the *AAVS1* safe-harbor locus. We used this system to compare rescue of cell viability and telomere length by wild-type versus RAP-compromised TERTs (Fig 6A). Transgenes expressing an untagged TERT were targeted, selected, and confirmed for integration at *AAVS1* as described previously, with TERT expression under control of the constitutive CAGGS promoter (Vogan *et al*, 2016). $TERT^{-/-}$ cells with only the selection marker integrated at *AAVS1* ceased proliferating and underwent cell death with reproducible timing. Cells expressing the thumb-helix K981E and the T-motif loop *Tetrahymena* sequence substitution also ceased proliferating and underwent cell death with the same timing as selection marker alone in three independent experimental replicates. We infer that complete lack of RAP at physiological dNTP concentrations precluded human telomerase maintenance of telomeres.

Cell cultures expressing wild-type, thumb-helix L980A, and motif 3 L681E TERTs all avoided cell death, with stably extended proliferative capacity and no difference in population doubling rate. We assayed whole-cell extracts of these cell cultures for telomerase activity using the PCR-based telomeric-repeat amplification protocol (TRAP). Amplified products of telomerase extension were biased to shorter lengths for the RAP-deficient TERT enzymes (Fig 6B), consistent with the direct primer extension assays (Figs 1F and 3B and D), but product intensities were roughly comparable in level to wild-type telomerase TRAP products. Telomeres were maintained stably in cells expressing a RAP-compromised TERT, but telomere lengths were shorter than in the parental HCT116 cells or cells expressing wild-type TERT from *AAVS1* (Fig 6C).

To test whether increasing the cellular amount of a low-RAP telomerase would compensate for the RAP deficiency, we increased the expression of wild-type hTR in the HCT116 cells with TERT transgenes. Lentiviral integration of a wild-type hTR expression cassette increased hTR accumulation detected by Northern blot (Fig 6D; note that mature hTR often migrates as a doublet due to folding during gel electrophoresis). Telomerase activity assayed by TRAP increased with increased hTR expression (Fig 6E). Remarkably, even in cells with severely RAP-compromised telomerase enzymes, hTR overexpression resulted in dramatic telomere elongation (Fig 6F). We conclude that when telomerase enzyme level is increased, even a RAP-deficient telomerase subverts telomeres' ability to restrain elongation.

Template alignment-region mutations that reduce RAP still allow telomere maintenance

As a parallel approach, we tested the biological function of mutant hTRs with the template alignment-region substitution A54U, A55U,

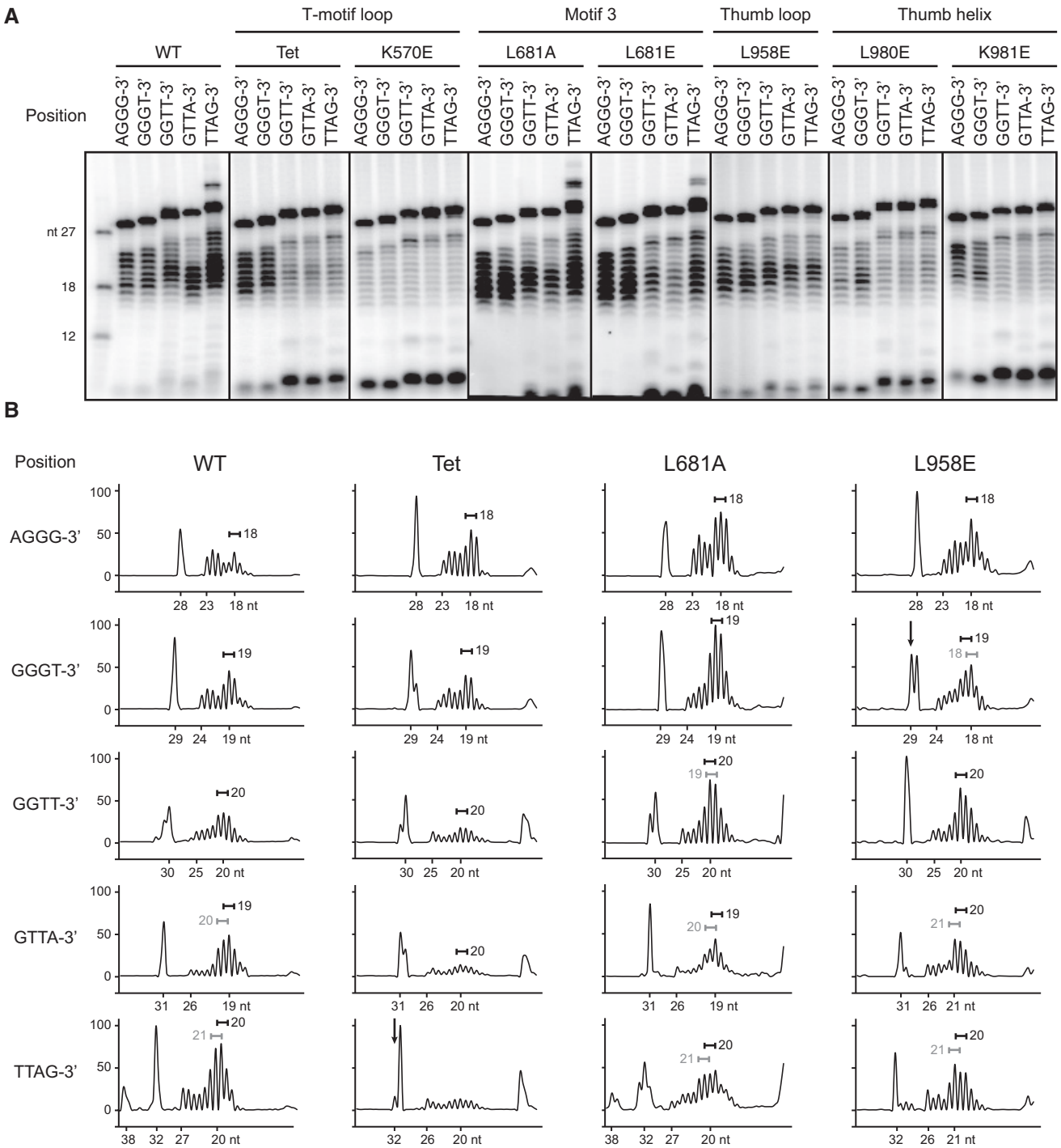

Figure 5. TERT motif substitutions have distinct consequences for product handling as synthesis proceeds to the template 5′ end.

A ExoVII protection assayed at each step of repeat synthesis for WT and TERT-mutant telomerases. Similar results were obtained in independent experimental replicates.

B Selected protected product profiles from (A) quantified by SAFA. Major and minor product peaks and lengths are indicated in black and gray, respectively. Protected product profiles of all TERT-mutant enzymes are shown in Fig EV3. Vertical arrow indicates the full repeat synthesis product when this product could be ambiguous.

or AA54-55UU (Fig 7A). These hTR mutations decrease RAP but do not change the sequence of telomeric-repeat synthesis (Drosopoulos *et al*, 2005). We assembled these hTR variants into telomerase holoenzymes to compare their impact on RAP. FLAG-tagged wild-type TERT and wild-type or mutant hTR were co-overexpressed by transient transfection of 293T cells (Fig 7B and C). Telomerase

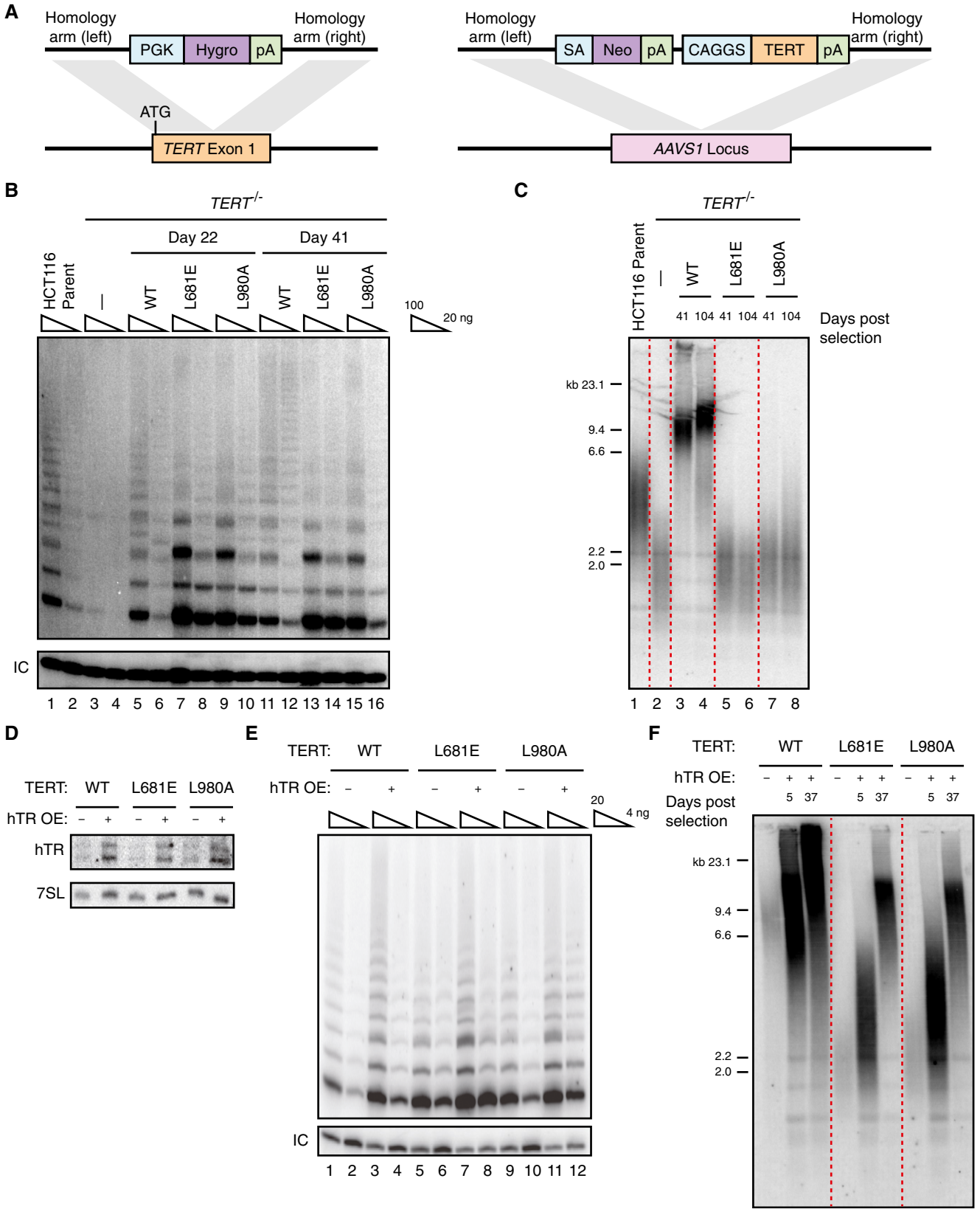

Figure 6.

Figure 6. Telomere maintenance or elongation by RAP-defective TERT-mutant telomerases.

A Schematic of gene editing strategy to test mutant-TERT function in HCT116 cells. After homozygous disruption of the endogenous *TERT* locus, a WT or mutant-TERT transgene is integrated at the *AAVS1* safe-harbor locus. Endogenous *TERT* knockout ($TERT^{-/-}$) and subsequent *TERT* transgene integration were selected using hygromycin (Hygro) and neomycin (Neo) resistance cassettes, respectively. PGK and CAGGS are promoters of transcription, pA indicates an mRNA polyadenylation signal, and SA indicates a splice acceptor motif.

B TRAP assay detection of telomerase activity in the HCT116 parental cells, $TERT^{-/-}$ cells, and $TERT^{-/-}$ cells with WT or mutant-TERT transgene. Whole-cell extract was normalized by total protein concentration and assayed at 100 or 20 ng total protein per TRAP reaction. $TERT^{-/-}$ cells were sampled at least 1 week prior to the onset of short-telomere-induced cell death. Other cells were sampled at 22 and 41 days after neomycin selection for transgene integration; parallel results were obtained for cells sampled at a third time point after selection (data not shown). Here and in subsequent TRAP assay panels, detection of the internal control (IC) PCR amplification product is shown.

C Telomere restriction fragment analysis of HCT116 parental cells, $TERT^{-/-}$ cells, and $TERT^{-/-}$ cells with a WT or mutant-TERT transgene. $TERT^{-/-}$ cells were sampled at least 1 week prior to the onset of short-telomere-induced cell death; these cells had ceased proliferating and underwent cell death substantially prior to the transgene-expressing cells' time point of 41 days post-selection. Transgene-expressing cells were viable when discontinued in culture at 172 days post-selection.

D Northern blot detection of hTR in HCT116 $TERT^{-/-}$ cells with WT or mutant-TERT transgene, with or without stable overexpression of hTR. The signal recognition particle 7SL RNA was detected as a loading control. Note that full-length hTR often migrates as a doublet due to partial folding during denaturing acrylamide PAGE.

E TRAP assay detection of telomerase activity in HCT116 cells with WT or mutant TERT and with or without stable overexpression of hTR. Whole-cell extract was normalized by total protein concentration and assayed at 20 or 4 ng total protein per TRAP reaction. Cells with overexpression of hTR were sampled at 5 days after puromycin selection for lentiviral integration; parallel results were obtained for selected cells sampled at a later time point after selection (data not shown).

F Telomere restriction fragment analysis of HCT116 $TERT^{-/-}$ cells with WT or mutant-TERT transgene, with or without stable overexpression of hTR. Cells without hTR overexpression were sampled approximately 2 months after selection for the *TERT* transgene. Cells with hTR overexpression were sampled at the indicated days of post-selection culture.

Data information: For all of the Fig 6 panels, similar results were obtained in independent experimental replicates.

holoenzyme was purified from cell extract by binding to FLAG-antibody resin and assayed for repeat synthesis activity using end-labeled primer at near-physiological and elevated dNTP concentrations. In either condition, the rank order of holoenzyme RAP was wild-type > A55U > A54U > AA54-55UU hTR telomerase (Fig 7D).

Homozygous disruption of the endogenous hTR locus ($TERC^{-/-}$) in HCT116 cells leads to progressive telomere shortening and short-telomere-induced cell death on the same schedule as $TERT^{-/-}$, rescued by wild-type hTR expression from *AAVS1* (Vogan *et al*, 2016). We compared rescue of cell viability and telomere length by wild-type hTR versus the alignment-region hTR mutants using the U3 snoRNA promoter to drive hTR expression in an integrated transgene (Fig 7E). Transgenes were targeted, selected, and confirmed for integration as described previously (Vogan *et al*, 2016). All of the transgene-encoded hTRs (wild-type, A54U, A55U, AA54-55UU) rescued $TERC^{-/-}$ cell death, conferring stably extended proliferative capacity.

Proliferating cells expressing transgene hTR detected by Northern blot (Fig 7F) gained telomerase activity assayed by TRAP (Fig 7G). Amplified products of telomerase extension were biased to shorter lengths by the A54U and AA54-55UU hTR alignment-region mutations (Fig 7G, lanes 7–8 and 11–12), consistent with the direct primer extension assays (Fig 7D). The $TERC^{-/-}$ cells rescued by wild-type hTR expression gained telomere length, eventually exceeding telomere lengths in the parental HCT116 cell line (Fig 7H, lanes 1–4). Surprisingly, telomere lengths were only slightly if at all shorter in cells expressing transgene A55U hTR than in cells expressing transgene wild-type hTR (Fig 7H, compare lanes 7–8 to lanes 3–4), despite RAP deficiency (Fig 7D, compare lane 1–3 or 5–7). Cells expressing A54U hTR also gained telomere length, but in a clearly compromised manner (Fig 7H, lanes 5–6), and cells expressing hTR AA54-55UU experienced slight telomere shortening during extended long-term culture (lanes 9–10). We conclude that modest RAP compromise had no striking impact on telomerase function at

Figure 7. Mutations in the hTR template alignment region compromise RAP but support telomere maintenance.

A Schematic of the template alignment-region substitutions and their predicted impact on product–template base-pairing for synthesis halted at the template 5′ end (pre-translocation) and at the beginning of next-repeat synthesis (post-translocation). Base-pairs shown in light blue for the WT enzyme post-translocation are affected by the alignment-region mutations.

B Northern blot detection of WT or mutant hTR overexpressed with FLAG-tagged TERT in 293T cells. The 7SL RNA is detected as a total RNA loading control. Note that full-length hTR often migrates as a doublet due to partial folding during denaturing acrylamide PAGE.

C Immunoblot detection of FLAG-tagged TERT in the same cell extracts tested for hTR level in (B). Tubulin was detected as an extract loading control.

D Activity of WT or mutant hTR telomerase enriched from extracts tested in (B) and (C) by FLAG-antibody resin, assayed using the single-turnover assay with approximately physiological (10 μM) or high (250 μM) dNTP concentration.

E Schematic of gene editing strategy to test mutant hTR function in HCT116 cells. After homozygous disruption of the endogenous *TERC* (hTR) locus, a WT or mutant hTR transgene was integrated at the *AAVS1* safe-harbor locus. *TERC* knockout ($TERC^{-/-}$) and subsequent selection for hTR transgene integration were conducted using puromycin and neomycin resistance cassettes, respectively.

F Northern blot detection of hTR in the HCT116 parental cells, $TERC^{-/-}$ cells, and $TERC^{-/-}$ cells with an integrated WT or mutant hTR transgene. Note that full-length hTR often migrates as a doublet due to partial folding during denaturing acrylamide PAGE.

G TRAP assay detection of telomerase activity in the HCT116 parental cells, $TERC^{-/-}$ cells, and $TERC^{-/-}$ cells with an integrated WT or mutant hTR transgene. Cells were sampled at 24 days after neomycin selection for transgene integration; parallel results were obtained for cells sampled at a subsequent time point (data not shown).

H Telomere restriction fragment analysis of HCT116 parental cells, $TERC^{-/-}$ cells, and $TERC^{-/-}$ cells with WT or mutant hTR transgene integration. $TERC^{-/-}$ cells were sampled at least 1 week prior to the onset of short-telomere-induced cell death; these cells had ceased proliferating at the transgene-expressing cells' time point of 18 days post-selection. Transgene-expressing cells were viable until eventually discontinued in culture at 151 days post-selection.

Data information: Similar results were obtained in independent experimental replicates.

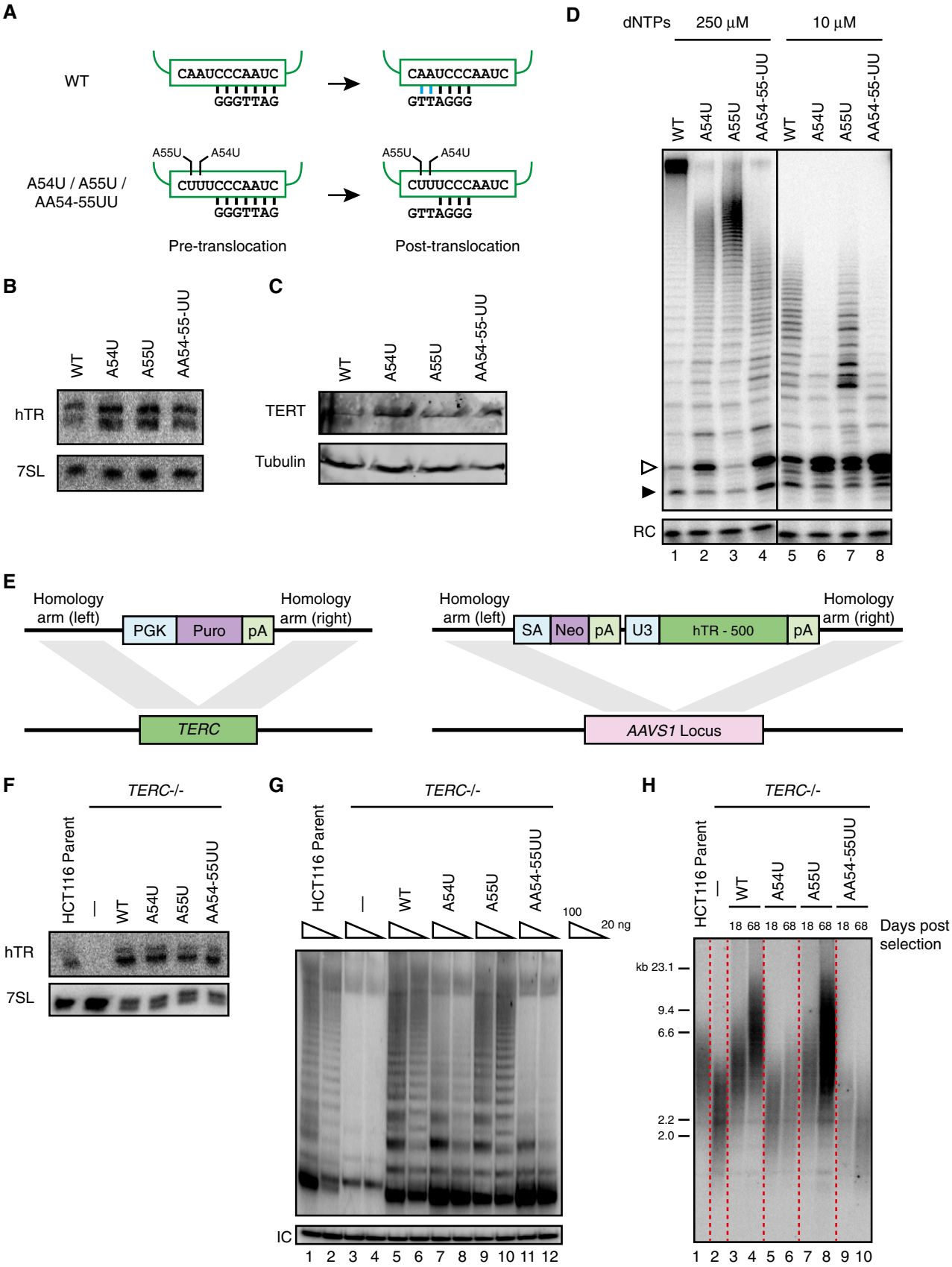

Figure 7.

telomeres, and even severe RAP compromise did not preclude telomerase from stable maintenance of short telomeres. Together, the biological activities of TERT- and hTR-mutant telomerases at telomeres implicate RAP as a determinant of telomere length. Within upper and lower bounds, human telomerase RAP influences the telomere length set point for homeostasis. Some RAP compromise can occur without notable phenotype, but complete loss of RAP appears incompatible with human telomere maintenance.

Discussion

In this work, we combined biochemical and cellular assays to determine the structural basis and biological roles of human telomerase RAP. Chemical inhibition has implicated human telomerase RAP as a contributor to telomere length (Pascolo *et al*, 2002). Two disease-associated human TERT mutations that decrease telomerase function correlatively decrease RAP (Robart & Collins, 2010; Zaug *et al*, 2013), but other consequences of these TERT mutations for nucleic acid handling were not tested. Here, enabled by a high-resolution structure of *Tribolium* TERT bound to a DNA–RNA duplex (Mitchell *et al*, 2010), a physical assay for product DNA handling by active enzyme (Wu & Collins, 2014), and screening of over 100 side-chain substitutions in the TERT-specific motifs lining the active-site cavity, we resolved changes in product DNA handling at each template position and their dependence on side chains in the TERT active-site cavity (Fig 8A). The telomerase catalytic-cycle transitions through states with many specializations of nucleic acid handling required for processive repeat synthesis. Specific interactions define the TER region used as template (Fig 8B, states 5 and 1), allow stable active-site engagement of the short duplex formed at the template 3′ end (states 1–2), dissociate duplex at the template 5′ end (states 4–6), and retain ssDNA during template translocation (states 6–7). Here, we sought to understand the structural principles of duplex and ssDNA recognition and their relevance to telomerase function at telomeres.

Dynamics and structural principles of duplex handling

As a framework for integrating the results of this work and previous studies, we suggest that during synthesis across the internal template, human telomerase stabilizes and protects a varying length of DNA–RNA duplex (Fig 4E) and about two repeats of ssDNA exiting the RNP from the active-site cavity. The changes in exonuclease-protected product lengths during synthesis across the template fit the model of a maximal duplex length of about seven base-pairs, which implies a loss of template 3′ end pairing prior to synthesis at the template 5′ end. We disfavor the alternate hypothesis that changes in protected product lengths reflect altered duplex positioning without any template unpairing, based on results from assays using the CCCAGG-3′ primer (Fig 4F) and precedent from budding yeast (Förstemann & Lingner, 2005).

Telomerase reverse transcriptase mutations in the T-motif loop and thumb helix increased DNA dissociation preferentially upon synthesis to GGTT-3′. It seems paradoxical that duplex stabilization is selectively compromised as primer is extended toward the template 5′ end, given that duplex length appears to increase with synthesis. Because the TEN domain is critical for short duplex stabilization (Jurczyluk *et al*, 2011; Wu & Collins, 2014; Akiyama *et al*, 2015), we suggest that mid-template duplexes with AGGG-3′ and GGGT-3′ are stabilized by the TEN domain and TERT ring RNP collaboratively. Then, upon synthesis to GGTT-3′ or beyond, duplex stabilization derives primarily or exclusively from the active-site cavity of the TERT ring. This shift could contribute to the product 3′ end permutation dependence of off-rate from human telomerase, which decreases with synthesis to mid-template and then increases with synthesis to the template 5′ end (Wallweber *et al*, 2003).

TERT-mutant enzymes with substitutions in the T-motif loop, thumb loop, and thumb helix all failed to unpair protected product from the template 3′ end upon synthesis of GTTA-3′. The T-motif loop, thumb loop, and thumb helix are deep within the active-site cleft (Fig 8A, left), where they could discriminate the sequence of the final base-pairs of template 5′ end duplex to execute sequence-specified template 5′ boundary definition (Brown *et al*, 2014). Our findings suggest that recognition of duplex base-pairs toward the template 5′ end influences fraying of base-pairs toward the template 3′ end. TERT interaction with template-frayed ssDNA as well as the product–template duplex DNA strand would create a large surface for ssDNA retention in RAP (see below).

Telomerase with A54U hTR had enhanced product dissociation after synthesis to GGGT-3′ (Fig 7D, lane 2; note the relatively strong products at +3 as well as +6 in each repeat, which are even more severe for AA54-55UU hTR holoenzyme in lane 4). This change was not ameliorated by high dNTP concentration in the activity assay reaction. The profile of product release by A54U hTR enzyme supports the model that duplex length for GGGT-3′ product includes base-pairing of A54 (Fig 4E). We note that initial base-pairing of a DNA 3′ end with the template alignment region (Fig 8B, state 1) could be more extensive than that detected for

Figure 8. New models for product–template duplex interaction and ssDNA retention enabling human telomerase RAP.

A TERT side chains that can contact the DNA strand (left panel) or RNA strand (right panel) of product–template duplex are colored and labeled in orange for the crystalized *Tribolium* protein (TcTERT), with the corresponding human TERT (hTERT) amino acids also indicated (PBD accession code 3KYL) (Mitchell *et al*, 2010). The entire T-motif loop is also colored orange to indicate possible nucleic acid contacts. The DNA strand is in blue, and the template strand is in green. The SRS side chains are positioned to interact with the DNA strand (left panel), whereas motif 3 is nearest to the RNA strand (right panel).

B Active-site binding of the template 3′ end duplex triggers active-site closure for elongation (states 1–2). When product is extended by synthesis toward the template 5′ end, duplex fraying occurs at the template 3′ end (states 4–5). Opening of the active-site cavity allows the template RNA strand to dissociate from SRS-bound ssDNA and reposition (states 6–7).

C The SRS (red) makes multiple contributions to DNA strand handling depending on the length of the duplex and the conformation of the active-site cavity. Motif 3 (orange) may facilitate template repositioning for formation of the template 3′ end duplex. The DNA strand is in blue, the template strand is in green, and TERT ring is in gray with CTE and RT domains indicated. Additional detail is in the main text.

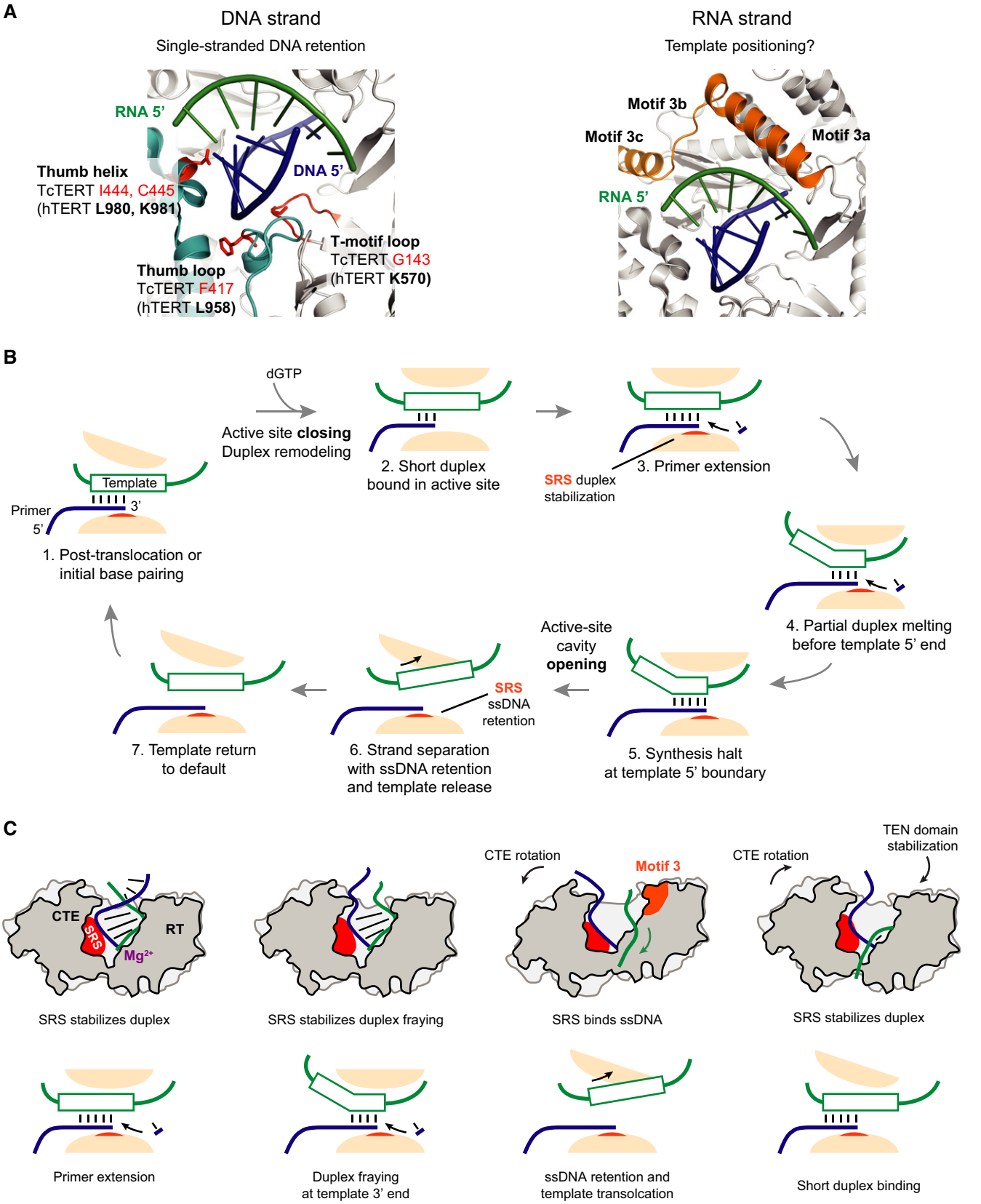

Figure 8.

product AGGG-3′ (Fig 8B, state 2), for example, if the base-pairs formed at the extreme template 3′ end exist transiently prior to DNA extension.

Curiously, in HCT116 cells, A55U hTR holoenzyme elongated telomeres as well as wild-type holoenzyme despite substantial reduction of RAP (Fig 7H). We speculate that the full RAP inherent to telomerase holoenzyme is not necessary to generate the length of product ssDNA that promotes telomerase termination by other ssDNA binding proteins (Chen *et al*, 2012; Wan *et al*, 2015). Also, telomere-associated proteins such as TPP1 could compensate for the hTR A55U mutation as part of their biological role in telomerase activation (Hockemeyer & Collins, 2015).

From duplex to ssDNA then back: overlapping, inter-convertible duplex and ssDNA binding sites for the product 3′ end

Despite considerable investigation, the physical basis of telomerase's template-independent ssDNA product retention has remained mysterious. Although ssDNA 5′ of a template-paired primer region improves primer binding affinity, RAP does not depend on this ssDNA (Hardy *et al*, 2001; Baran *et al*, 2002; Wallweber *et al*, 2003). Recent precedent for how product 3′ end realignment can occur within a polymerase active site provides a solution for one telomerase conundrum: How can an active site that snuggly fits duplex reposition one strand without loss of the other? By outward rotation of the polymerase thumb domain (the telomerase CTE), the active site could open to allow displacement of one strand relative to the other (Yang & Lee, 2015). In the case of polymerase ν, this rotation allows the primer strand of the product–template duplex to slip backward (Lee *et al*, 2015). For telomerase, we suggest that the DNA strand remains bound to the outward-rotated CTE while the template strand slips, allowing the template 3′ end to relocate to where it could be recaptured by the ssDNA 3′ end (Fig 8B, state 5 to 1; Fig 8C). This scenario is consistent with competition of a six- or eight-nucleotide RNA template oligonucleotide but not a complementary DNA oligonucleotide for next-repeat synthesis (Qi *et al*, 2012). The large conformational change of CTE outward rotation could be stimulated by the presence of template 5′ end duplex in the active site. Synthesis-dependent hTR movement modeled from single-molecule FRET recordings (Parks *et al*, 2017) may detect the outward rotation. Reversion to the inward-rotated CTE could be favored by template repositioning, prior to new duplex formation, because the *Tribolium* TERT ring has a pre-formed active-site cavity that closes only slightly upon occupancy with duplex (Mitchell *et al*, 2010) and so is presumably in the CTE "inward rotation" state (Yang & Lee, 2015).

The side chains L958, L980, and K981 of the TERT thumb-loop and thumb-helix cluster along a continuous surface (Fig 8A, left) adjacent to the primer strand in the *Tribolium* TERT structure with bound duplex (Mitchell *et al*, 2010). The T-motif loop conformation is not determined at atomic resolution, but its general location suggests that it could clamp around the DNA 3′ end on the face opposite the thumb helix to stabilize bound duplex (Fig 8A, left). Duplexes with product extended to the template 5′ end are indeed binding-stabilized by the T-motif loop and thumb helix, but not by the thumb loop, based on the TERT-mutant enzymes' relative turnover (Fig 2, pulse–chase primer elongation) and relative product dissociation (Fig 5, exonuclease protection). Destabilization of duplex binding alone would not account for loss of RAP, because product profiles indicate substantial amounts of complete-repeat product that could have been realigned with the template for next-repeat addition. All of the thumb-helix and thumb-loop substitutions at least partially failed to unpair template-product duplex, based on the profile of the exonuclease-protected products. Increased product dissociation from the thumb-helix TERT-mutant enzymes could hide some occurrence of template 3′ end fraying, but the thumb-loop L958A TERT-mutant enzyme with no increase in product dissociation also failed to unpair the template 3′ end prior to maximal duplex length.

We propose that the thumb loop and thumb helix along with the T-motif loop contribute to a ssDNA retention surface (SRS) that overlaps the binding surface for the DNA strand of template duplex (Fig 8C). During the CTE rotation that opens the active-site cavity and destabilizes duplex pairing, the SRS would retain the DNA strand of duplex as ssDNA. If the SRS is localized entirely to surfaces of the CTE, the ssDNA would be carried with it. In addition to the DNA strand of the template 5′ end duplex, the SRS could bind ssDNA frayed from the template 3′ end to favor template 3′ duplex unpairing. Furthermore, to reestablish product 3′ end base-pairing after template repositioning, an SRS-bound DNA 3′ end could base-pair to the template 3′ end without dissociation from the SRS, since at least part of the SRS can accommodate DNA–RNA duplex. SRS–DNA association may be reflected in the single-molecule FRET assays that detected two discrete positional states for the DNA nucleotide paired to the template 3′ end (Parks & Stone, 2014). With a template duplex of product GGGT-3′, only one state was detected; at product GTTA-3′ and TTAG-3′, roughly half or almost all of the DNA, respectively, was positioned in a second state (Parks & Stone, 2014). The shift in DNA position occurring at GTTA-3′ was less complete in the FRET assay than when assayed by exonuclease protection, consistent with an equilibrium that gives the exonuclease transient access to all bound product DNA. It will be of high interest to investigate how the two-state DNA positioning monitored by FRET is altered by TERT mutations that compromise SRS function.

We found that motif 3 TERT-mutant enzymes had unperturbed handling of product–template duplexes in the active site (Fig 5). Enzymes with motif 3 TERT mutations retain more RAP than the others tested for altered product–template duplex handling, but a qualitative as well as quantitative difference in duplex handling is likely due to motif 3 distance from the active site and positioning near the template strand of duplex (Fig 8A, right). We speculate that motif 3 contribution(s) to RAP occur through influence on RNA conformation rather than DNA binding. For example, motif 3 could promote template repositioning and formation of the realigned template 3′ end duplex (Fig 8C). This role would be consistent with the 5- to 10-fold increased K_m for a short DNA primer measured for L681A, G682A, and I686A TERT enzymes reconstituted *in vitro* (Xie *et al*, 2010). Also, a template release and repositioning function for motif 3 would account for why this motif is down-sized in TERTs from organisms likely to have non-processive repeat synthesis (Xie *et al*, 2010) including *Tribolium* TERT (Fig EV1).

The model presented here relies on dynamic nucleic acid recognition. First, DNA synthesis pushes the product–template duplex up the active-site cavity wall until its "tail" at the template 3′ end

frays (Fig 8B, states 3–5). Second, SRS–DNA contacts created or stabilized upon full repeat synthesis compete for template base-pairing (Fig 8B, states 5–6). Third, SRS-bound ssDNA provides the platform for recruiting the released template back to active-site engagement (Fig 8B, states 1–2). From this perspective, protein–DNA interaction rather than RNA strain could be the major thermodynamic driver of duplex unpairing, with RNA interactions playing a more critical role after template unpairing to confer favorable positioning of the template 5′ end for primer 3′ end base-pairing.

Human telomerase RAP in telomere elongation and maintenance

Previous studies point to an influence of RAP on human telomerase function at telomeres (Pascolo *et al*, 2002; Robart & Collins, 2010; Zaug *et al*, 2013). However, across organisms, the number of repeats that telomerase adds to a chromosome end is not correlated with telomerase RAP *in vitro*. Furthermore, across telomeres in a cell, telomerase RAP may differ with telomere length (Chang *et al*, 2007; Zhao *et al*, 2011). These observations raise the question of whether there is physiological significance to a specific level of inherent telomerase RAP assayed *in vitro*.

Here, we found that TERT-mutant human telomerases completely lacking RAP were unable to offset telomere shortening with proliferation or rescue short-telomere-induced cell death. Of more interest, we found that telomerases with severely reduced RAP could support short-telomere length homeostasis. At homeostasis, telomerase must restore the full length of sequence lost to genome replication and DNA damage. Thus, a low-RAP human telomerase can synthesize an end-protective overhang length on all or almost all telomeres in every cell cycle. Our previous studies demonstrated a similar short-telomere homeostasis in cells with altered TPP1 or very low levels of telomerase with normal RAP (Sexton *et al*, 2014; Vogan *et al*, 2016).

If critically short telomeres have a uniquely increased efficiency of telomerase recruitment, they could be refractory to net telomere elongation: If net elongation produced a slightly longer telomere, it might no longer have the structure that necessitates telomerase recruitment. We therefore tested whether low-RAP telomerase could accomplish net telomere elongation when overexpressed. In HeLa cells and human embryonic stem cells, telomerase overexpression induces dramatic and continuous telomere elongation apparently unlinked from feedback by telomere length (Cristofari & Lingner, 2006; Chiba *et al*, 2015). Likewise, in the HCT116 cells used in this work, telomerase overexpression induced a rapid and dramatic gain of telomere length (Fig 6F). Contrary to our expectation, even RAP-compromised telomerase could extend telomeres to longer lengths than in the parental cell line (Fig 6F). We suggest that high human telomerase enzyme abundance per se inhibits negative feedback regulation by telomere length even if telomerase has severely compromised RAP. As one possible mechanism, saturation binding of telomerase to TPP1 could antagonize the role of other TPP1-associated proteins in sequestering a chromosome 3′ end. Overall, our findings support the biological necessity of human telomerase RAP and the necessity for high RAP in the maintenance of long telomeres. In addition, independent of telomerase RAP, a cellular limit on active telomerase RNP level appears necessary for normal telomere length homeostasis.

Materials and Methods

Telomerase reconstitution

For reconstitution in RRL, TERT was expressed from pCITE-3xFLAG-TERT in the TNT T7-coupled transcription/translation kit according to the manufacturer's instructions (Promega) in the presence of purified *in vitro* transcribed hTRmin. Reactions were incubated at 30°C for 3.5 h. For reconstitution in cells, human 293T cells were transiently transfected with the TERT expression construct pcDNA3.1-3xFLAG-TERT and the hTR expression construct pBS-U3-hTR-500 using calcium phosphate. Media were changed after 24 h, and cells were harvested and lysed after 48 h by resuspension in hypotonic lysis buffer (20 mM HEPES pH 8, 2 mM $MgCl_2$, 0.2 mM EGTA, 10% glycerol, 0.1% NP-40, 1 mM DTT, and 0.1 mM PMSF) followed by three freeze–thaw cycles. The lysate was brought to 400 mM NaCl and cleared by centrifugation at 20,000 *g* at 4°C for 15 min. The cleared extract was adjusted to a final concentration of 150 mM NaCl.

Telomerase activity assays

Activity assays of telomerase reconstituted in 293T cells were performed after telomerase enrichment by binding to FLAG M2 monoclonal antibody resin (Sigma-Aldrich) in reaction buffer (50 mM Tris-acetate pH 8, 3 mM $MgCl_2$, 1 mM EGTA, 1 mM spermidine, 5 mM DTT, and 5% glycerol). For primer extension with radiolabeled dGTP, 500 nM 5′-$(T_2AG_3)_3$-3′ primer, 0.1 μM α-^{32}P dGTP (3,000 Ci/mmol, 10 mCi/ml, Perkin-Elmer), 250 μM dATP, 250 μM dTTP, and 5 μM dGTP were included. For extension of end-labeled primer, 5′ ^{32}P end-labeled $(T_2AG_3)_3$ primer was bound to immobilized telomerase at room temperature for 30 min. Unbound primer was removed by washing with hypotonic lysis buffer containing 150 mM NaCl, 0.1% Triton X-100, and 0.2% CHAPS. The immobilized telomerase was resuspended in reaction buffer containing 10 μM or 250 μM each of dATP, dCTP, dGTP, and dTTP. Reactions were incubated at 30°C for 40 min prior to extraction. For the pulse–chase primer extension assay, immobilized telomerase was allowed to bind 5′-$T_{21}GT_2AG_2$-3′ primer supplied at 50 nM at room temperature for 30 min. Reaction buffer containing 0.1 μM α-^{32}P dGTP was added and incubated at 30°C for 5 min. After the 5-min labeling period, 5′-$(T_2AG_3)_3$-3′ chase primer was added to a final concentration of 10 μM. Reactions were incubated at 30°C for the indicated reaction duration. The products of all primer extension reactions were extracted, precipitated, and resolved by denaturing PAGE. A ^{32}P end-labeled oligonucleotide was added prior to product precipitation as a recovery control. Various ^{32}P end-labeled primers were used as size markers. Gels were dried and products detected by phosphorimaging on a Typhoon Trio system (GE Healthcare).

Activity assays from whole-cell extract were performed by TRAP. Telomerase extension of the oligonucleotide TS (5′-AATCCGTCGAG CAGAGTT-3′) was detected by PCR amplification of products using TS and primer ACX (5′-GCGCGGCTTA$(C_3T_2A)_2$CCCTAACC-3′). The internal control was oligonucleotide TSNT (5′-AATCCGTCGAGCAG AGTTAAAAGGCCGAGAAGCGAT-3′) amplified by primers ACX and NT (5′-ATCGCTTCTCGGCCTTTT-3′). PCR was carried out by 28 cycles of 30-s incubations alternating between 94 and 60°C with Taq polymerase in the presence of α-^{32}P dGTP. Products were resolved

on native 10% (19:1 acrylamide:bis-acrylamide) 0.5× Tris borate–EDTA gels. Gels were dried and products detected by phosphorimaging on a Typhoon Trio system (GE Healthcare).

Exonuclease protection assays

Telomerase immobilized on FLAG-antibody resin was allowed to bind 5′-$T_{21}GT_2AG_2$-3′ primer supplied at 1 μM and incubated at room temperature for 30 min. Primer extension was initiated by addition of reaction buffer and a final concentration of 0.1 μM α-^{32}P dGTP and, if included, 250 μM dATP, 250 μM dTTP, and/or 500 μM of ddNTP. Reactions were incubated at room temperature for 1 min, followed by addition of five units of ExoVII (Affymetrix). Reactions were further incubated at room temperature for 5 min. Products were extracted, precipitated, and resolved by denaturing PAGE. ^{32}P end-labeled oligonucleotides were loaded as size markers. Gels were dried and visualized by phosphorimaging on a Typhoon Trio system (GE Healthcare). Products were quantified using semi-automated footprinting analysis (SAFA) software version 11b (Das *et al*, 2005). A triplet of nuclease-protected product lengths was assumed for each DNA position. In cases of four consecutive prominent product lengths, we suggest two triplets labeled as major or minor based on the triplet peaks and triplet-flanking product intensities.

HCT116 cell culture and genome editing

HCT116 cells were cultured in DMEM with GlutaMax (Thermo) supplemented with 10% FBS and 100 μg/ml Primocin (Invivogen). Clonal cell lines with homozygous TERT or TERC disruption were generated previously (Vogan *et al*, 2016). Conditions of HCT116 gene targeting and selection were previously described (Vogan *et al*, 2016). The method for transgene integration at *AAVS1* was also previously described (Sexton *et al*, 2014). Cells selected for transgene integration were maintained as polyclonal cultures, because any non-integrant cells were removed by selection for culture growth past the time interval when the parental homozygous TERT- or TERC-disruption cells underwent cell death. Lentiviral infection for hTR overexpression was done using cells cultured continuously for > 3 months after selection for integration of a TERT transgene.

Lentivirus was produced in 293T cells by calcium phosphate transfection with the packaging plasmid, psPAX2, the envelope plasmid, pMD2.G, with transgene constructs in the DUET011 backbone (Zhou *et al*, 2007). The hygromycin resistance cassette was replaced by a puromycin resistance cassette. Cell transfection media were replaced at 24 h post-transfection, and virus was harvested 48 h post-transfection. Virus-containing media were applied to HCT116 cells in the presence of 5 μg/ml polybrene (Sigma) for 24 h before media change. At 48 h post-infection, cells were selected with 1 μg/ml puromycin.

Northern and Southern blotting

RNA was purified using TRIzol reagent (Life Technologies) and resolved on 5% (19:1 acrylamide:bis-acrylamide), 0.6× Tris borate-EDTA, 7 M urea gels. RNA was transferred onto Hybond N+ nylon membrane (GE Healthcare), UV-cross-linked, and incubated with Church's buffer (1% BSA, 1 mM EDTA, 0.5 M $NaPO_4$, 7% SDS) with 15% formamide at 50°C for 3 h. End-radiolabeled probe complementary to 3′ template-flanking nucleotides of hTR or 7SL RNA were added and incubated at 50°C overnight. Membranes were washed twice at 50°C for 20 min with 1× SSC + 0.1% SDS, and signal was visualized by phosphorimaging on a Typhoon Trio system (GE Healthcare). Genomic DNA was prepared, digested with MboI and AluI, and probed for telomeric repeats with ^{32}P end-labeled 5′-$(T_2AG_3)_3$-3′ as described (Vogan *et al*, 2016).

Immunoblotting

Proteins were resolved on 10% SDS–PAGE gels and transferred to nitrocellulose membranes. Membranes were incubated in 5% non-fat milk (Carnation) in Tris-buffered saline (TBS) buffer (150 mM NaCl, 50 mM Tris pH 7.5) at room temperature for 1 h, followed by incubation with primary antibodies diluted in 3% non-fat milk in TBS buffer at 4°C overnight. FLAG-tagged TERT was detected using mouse anti-FLAG monoclonal primary antibody F1804 (Sigma-Aldrich) at 1:4,000 dilution, and tubulin was detected using mouse anti-α-tubulin monoclonal primary antibody DM1A (Calbiochem) at 1:500 dilution. Membranes were extensively washed with TBS buffer, followed by secondary antibody incubation with goat anti-mouse IR 800 antibody A-14 (Santa Cruz Biotechnology) at 1:3,000 dilution in 3% non-fat milk in TBS buffer at room temperature for 45 min. After extensive washing with TBS buffer, immunoblots were imaged on a LI-COR Odyssey imager (LI-COR Biosciences).

Expanded View for this article is available online.

Acknowledgements

We thank Jacob Vogan and Xiaozhu Zhang for HCT116 cells including the *TERT*$^{-/-}$ and *TERC*$^{-/-}$ lines, expression constructs, and assistance with cell culture experiments. We also thank Aishwarya Deshpande, Heather Upton, and Jacob Vogan for comments on the manuscript. This work was supported by N.I.H. grants GM054198 and HL079585 to K.C.

Author contributions

RAW performed the experiments with telomerase reconstituted in RRL or by expression in 293T cells. JT performed the HCT116 cell culture experiments. RAW and KC designed the experiments and prepared the manuscript. All authors contributed to result analysis and manuscript revision.

Conflict of interest

The authors declare that they have no conflict of interest.

References

Akiyama BM, Parks JW, Stone MD (2015) The telomerase essential N-terminal domain promotes DNA synthesis by stabilizing short RNA-DNA hybrids. *Nucleic Acids Res* 43: 5537 – 5549

Arnoult N, Karlseder J (2015) Complex interactions between the DNA-damage response and mammalian telomeres. *Nat Struct Mol Biol* 22: 859 – 866

Baran N, Haviv Y, Paul B, Manor H (2002) Studies on the minimal lengths required for DNA primers to be extended by the *Tetrahymena* telomerase: implications for primer positioning by the enzyme. *Nucl Acids Res* 30: 5570 – 5578

Blackburn EH, Greider CW, Szostak JW (2006) Telomeres and telomerase: the path from maize, *Tetrahymena* and yeast to human cancer and aging. *Nat Med* 12: 1133 – 1138

Brown AF, Podlevsky JD, Qi X, Chen Y, Xie M, Chen JJ (2014) A self-regulating template in human telomerase. *Proc Natl Acad Sci USA* 111: 11311 – 11316

Chang M, Arneric M, Lingner J (2007) Telomerase repeat addition processivity is increased at critically short telomeres in a Tel1-dependent manner in *Saccharomyces cerevisiae*. *Genes Dev* 21: 2485 – 2494

Chen LY, Redon S, Lingner J (2012) The human CST complex is a terminator of telomerase activity. *Nature* 488: 540 – 544

Chiba K, Johnson JZ, Vogan JM, Wagner T, Boyle JM, Hockemeyer D (2015) Cancer-associated TERT promoter mutations abrogate telomerase silencing. *eLife* 4: e07918

Cristofari G, Lingner J (2006) Telomere length homeostasis requires that telomerase levels are limiting. *EMBO J* 25: 565 – 574

Damm K, Hemmann U, Garin-Chesa P, Hauel N, Kauffmann I, Priepke H, Niestroj C, Daiber C, Enenkel B, Guilliard B, Lauritsch I, Muller E, Pascolo E, Sauter G, Pantic M, Martens UM, Wenz C, Lingner J, Kraut N, Rettig WJ *et al* (2001) A highly selective telomerase inhibitor limiting human cancer cell proliferation. *EMBO J* 20: 6958 – 6968

Das R, Laederach A, Pearlman SM, Herschlag D, Altman RB (2005) SAFA: semi-automated footprinting analysis software for high-throughput quantification of nucleic acid footprinting experiments. *RNA* 11: 344 – 354

Doksani Y, de Lange T (2014) The role of double-strand break repair pathways at functional and dysfunctional telomeres. *Cold Spring Harb Perspect Biol* 6: a016576

Drosopoulos WC, Direnzo R, Prasad VR (2005) Human telomerase RNA template sequence is a determinant of telomere repeat extension rate. *J Biol Chem* 280: 32801 – 32810

Drozdetskiy A, Cole C, Procter J, Barton GJ (2015) JPred4: a protein secondary structure prediction server. *Nucleic Acids Res* 43: W389 – W394

Förstemann K, Lingner J (2005) Telomerase limits the extent of base pairing between template RNA and telomeric DNA. *EMBO Rep* 6: 361 – 366

Gillis AJ, Schuller AP, Skordalakes E (2008) Structure of the *Tribolium castaneum* telomerase catalytic subunit TERT. *Nature* 455: 633 – 637

Greider CW (1991) Telomerase is processive. *Mol Cell Biol* 11: 4572 – 4580

Greider CW (2016) Regulating telomere length from the inside out: the replication fork model. *Genes Dev* 30: 1483 – 1491

Hardy CD, Schultz CS, Collins K (2001) Requirements for the dGTP-dependent repeat addition processivity of recombinant *Tetrahymena* telomerase. *J Biol Chem* 276: 4863 – 4871

Hockemeyer D, Collins K (2015) Control of human telomerase action at telomeres. *Nat Struct Mol Biol* 22: 848 – 852

Jurczyluk J, Nouwens AS, Holien JK, Adams TE, Lovrecz GO, Parker MW, Cohen SB, Bryan TM (2011) Direct involvement of the TEN domain at the active site of human telomerase. *Nucleic Acids Res* 39: 1774 – 1788

Lee YS, Gao Y, Yang W (2015) How a homolog of high-fidelity replicases conducts mutagenic DNA synthesis. *Nat Struct Mol Biol* 22: 298 – 303

Lin K, Simossis VA, Taylor WR, Heringa J (2005) A simple and fast secondary structure prediction method using hidden neural networks. *Bioinformatics* 21: 152 – 159

Lloyd NR, Dickey TH, Hom RA, Wuttke DS (2016) Tying up the ends: plasticity in the recognition of single-stranded DNA at telomeres. *Biochemistry* 55: 5326 – 5340

MacNeil DE, Bensoussan HJ, Autexier C (2016) Telomerase regulation from beginning to the end. *Genes* 7: 64

Maine IP, Chen S, Windle B (1999) Effect of dGTP concentration on human and CHO telomerase. *Biochemistry* 38: 15325 – 15332

Martinez P, Blasco MA (2015) Replicating through telomeres: a means to an end. *Trends Biochem Sci* 40: 504 – 515

Mitchell JR, Collins K (2000) Human telomerase activation requires two independent interactions between telomerase RNA and telomerase reverse transcriptase *in vivo* and *in vitro*. *Mol Cell* 6: 361 – 371

Mitchell M, Gillis A, Futahashi M, Fujiwara H, Skordalakes E (2010) Structural basis for telomerase catalytic subunit TERT binding to RNA template and telomeric DNA. *Nat Struct Mol Biol* 17: 513 – 518

Morin GB (1991) Recognition of a chromosome truncation site associated with alpha-thalassaemia by human telomerase. *Nature* 353: 454 – 456

Parks JW, Stone MD (2014) Coordinated DNA dynamics during the human telomerase catalytic cycle. *Nat Commun* 5: 4146

Parks JW, Kappel K, Das R, Stone MD (2017) Single-molecule FRET-Rosetta reveals RNA structural rearrangements during human telomerase catalysis. *RNA* 23: 175 – 188

Pascolo E, Wenz C, Lingner J, Hauel N, Priepke H, Kauffmann I, Garin-Chesa P, Rettig WJ, Damm K, Schnapp A (2002) Mechanism of human telomerase inhibition by BIBR1532, a synthetic, non-nucleosidic drug candidate. *J Biol Chem* 277: 15566 – 15572

Podlevsky JD, Bley CJ, Omana RV, Qi X, Chen JJ (2008) The telomerase database. *Nucleic Acids Res* 36: D339 – D343

Podlevsky JD, Chen JJ (2016) Evolutionary perspectives of telomerase RNA structure and function. *RNA Biol* 22: 204 – 215

Qi X, Xie M, Brown AF, Bley CJ, Podlevsky JD, Chen JJ (2012) RNA/DNA hybrid binding affinity determines telomerase template-translocation efficiency. *EMBO J* 31: 150 – 161

Robart AR, Collins K (2010) Investigation of human telomerase holoenzyme assembly, activity, and processivity using disease-linked subunit variants. *J Biol Chem* 285: 4375 – 4386

Robart AR, Collins K (2011) Human telomerase domain interactions capture DNA for TEN domain-dependent processive elongation. *Mol Cell* 42: 308 – 318

Sexton AN, Regalado SG, Lai CS, Cost GJ, O'Neil CM, Urnov FD, Gregory PD, Jaenisch R, Collins K, Hockemeyer D (2014) Genetic and molecular identification of three human TPP1 functions in telomerase action: recruitment, activation, and homeostasis set point regulation. *Genes Dev* 28: 1885 – 1899

Sun D, Lopez-Guajardo C, Quada J, Hurley LH, Von Hoff DD (1999) Regulation of catalytic activity and processivity of human telomerase. *Biochemistry* 38: 4037 – 4044

Vasianovich Y, Wellinger RJ (2017) Life and death of yeast telomerase RNA. *J Mol Biol* doi: 10.1016/j.jmb.2017.01.013

Vogan JM, Zhang X, Youmans DT, Regalado SG, Johnson JZ, Hockemeyer D, Collins K (2016) Minimized human telomerase maintains telomeres and resolves endogenous roles of H/ACA proteins, TCAB1, and Cajal bodies. *eLife* 5: e18221

Wallweber G, Gryaznov S, Pongracz K, Pruzan R (2003) Interaction of human telomerase with its primer substrate. *Biochemistry* 42: 589 – 600

Wan B, Tang T, Upton H, Shuai J, Zhou Y, Li S, Chen J, Brunzelle JS, Zeng Z, Collins K, Wu J, Lei M (2015) The *Tetrahymena* telomerase p75-p45-p19 subcomplex is a unique CST complex. *Nat Struct Mol Biol* 22: 1023 – 1026

Wang H, Blackburn EH (1997) *De novo* telomere addition by *Tetrahymena* telomerase *in vitro*. *EMBO J* 16: 866 – 879

Weinrich SL, Pruzan R, Ma L, Ouellette M, Tesmer VM, Holt SE, Bodnar AG, Lichsteiner S, Kim NW, Trager JB, Taylor RD, Carlos R, Andrews WH, Wright WE, Shay JW, Harley CB, Morin GB (1997) Reconstitution of human

telomerase with the template RNA component hTR and the catalytic protein subunit hTRT. *Nat Genet* 17: 498 – 502

Wu RA, Collins K (2014) Human telomerase specialization for repeat synthesis by unique handling of primer-template duplex. *EMBO J* 33: 921 – 935

Wu RA, Dagdas YS, Yilmaz ST, Yildiz A, Collins K (2015) Single-molecule imaging of telomerase reverse transcriptase in human telomerase holoenzyme and minimal RNP complexes. *eLife* 4: e08363

Wu RA, Upton HE, Vogan JM, Collins K (2017) Telomerase mechanisms of telomere synthesis. *Annu Rev Biochem* doi: 10.1146/annurev-biochem-061516-045019

Xie M, Podlevsky JD, Qi X, Bley CJ, Chen JJ (2010) A novel motif in telomerase reverse transcriptase regulates telomere repeat addition rate and processivity. *Nucleic Acids Res* 38: 1982 – 1996

Yang W, Lee YS (2015) A DNA-hairpin model for repeat-addition processivity in telomere synthesis. *Nat Struct Mol Biol* 22: 844 – 847

Yu G, Blackburn EH (1991) Developmentally programmed healing of chromosomes by telomerase in *Tetrahymena*. *Cell* 67: 823 – 832

Zaug AJ, Crary SM, Jesse Fioravanti M, Campbell K, Cech TR (2013) Many disease-associated variants of hTERT retain high telomerase enzymatic activity. *Nucleic Acids Res* 41: 8969 – 8978

Zhao Y, Abreu E, Kim J, Stadler G, Eskiocak U, Terns MP, Terns RM, Shay JW, Wright WE (2011) Processive and distributive extension of human telomeres by telomerase under homeostatic and nonequilibrium conditions. *Mol Cell* 42: 297 – 307

Zhou BY, Ye Z, Chen G, Gao ZP, Zhang YA, Cheng L (2007) Inducible and reversible transgene expression in human stem cells after efficient and stable gene transfer. *Stem Cells* 25: 779 – 789